

RESEARCH ARTICLE

Open Access

Sustainability problems of the Giza pyramids



Sayed Hemeda^{1*}  and Alghreeb Sonbol²

Abstract

The Pyramids complex in Giza consists of three main pyramids in addition to the famous Sphinx and small queen's pyramids. Recently, the pyramids of Cheops (Khufu), Chephren (Khafre) and Mykerinos (Menkaure) on the Giza plateau have been threatened by a rising groundwater table resulting from water leakage from the suburbs irrigation canals, and mass urbanization surrounding the Giza pyramids. The pyramids at Giza suffer from a lot of Geo-environmental and structural problems. The main objectives of this study are (1) to assess the current status of the preservation of this unique and high valuable archaeological site, (2) to analyze the various actions that cause the destruction of the pyramid complex, in particular the weathering activities and strong seismic event, and (3) to determine the geochemical and engineering properties for construction materials using different types of tools and advanced analytical and diagnostic techniques. Structural stability analysis requires good assessment of present conditions of major materials used such as stones and structural mortar. The paper shows a thorough analysis of the current condition of the Great Pyramids at Giza. The work includes a discussion and analysis of the natural character and source of the pyramids building stones, geological context, damage survey, petrographic investigation, and physical and mechanical characterization of the stones and structural mortars, by means of laboratory and in situ testing. The results are displayed, described and analyzed in the paper in the context of potential threats to the monuments. The experimental study indicates the dependence of mechanical geological properties on the physical properties and the mineral composition of the studied building materials. The physical and petrographic characteristic of the stones are related. The modeling of properties indicates a reliable relationship between the various visible pores and uniaxial compression force parameters that can be applied to predict and characterize limestone elsewhere.

Keywords: Pyramids at Giza, Great pyramid of Khufu, Building materials, Petrophysical properties, Geomechanical properties, Petrophysical properties, Sustainability

Introduction

The Pyramids of Giza are the largest and most famous pyramid structures in the world. It was built to honor some pharaohs of the Fourth Dynasty of Egypt during a period known as the Old Kingdom. The Old Kingdom was the first great era of Egyptian civilization and lasted from 2686 to 2181 BC.

Pyramids of Giza, fourth Dynasty (about 2575–2465 BC) pyramids were erected on a rocky plateau on the west bank of the Nile near Giza in northern Egypt. In ancient times, they were included in the Seven

Wonders of the ancient World. The ancient monuments of the Memphis region, including the Pyramids of Giza, Saqqara, Dahshur, Abu Rawash, were designated as a UNESCO World Heritage Site in 1979.

The Pyramids of Giza, built to endure forever, did exactly this. Archaeological tombs are remnants of the Old Kingdom of Egypt and were built about 4500 years ago.

Pharaohs thought in the resurrection, that there is a second life after death. To prepare for the next world, they set up temples of gods and huge pyramid tombs for themselves—filled with all the things each ruler would need to guide and preserve in the next world [1–3].

Pharaoh Cheops (Khufu) began the first project of the Pyramid of Giza, around 2550 BC. Its largest pyramid is the largest in Giza and is about 481 ft. (147 m)

*Correspondence: sayed.hemeda@cu.edu.eg

¹ Conservation Department, Faculty of Archaeology, Cairo University, P.O. 12613, Giza, Egypt

Full list of author information is available at the end of the article

high above the plateau. Its stone masses estimated at approximately 2.3 million, weigh an average of 2.5 to 15 tons. The great pyramid builders used stones of different sizes and heights for the different layers. The stone blocks of Khufu's pyramid were very large in the lower layers (1.0 m × 2.5 m base dimensions and 1.0–1.5 m high, 6.5–10 tons). For the layers that are higher up, it was easier to transport smaller blocks (1.0 m × 1.0 m × 0.5 m, appx 1.3 tons). For calculations most Egyptologists use 2.5 tons as the weight of an average pyramid stone block. 8000 tons of granite were imported from Aswan located at more than 800 km away. The largest granite stones in the pyramid, found above the “King's” chamber, weigh 25 to 80 tons each. About 500,000 tons of mortar was used in the construction of the great pyramid. Many of the casing stones and inner chamber blocks of the Great Pyramid were fit together with extremely high precision. Based on measurements taken on the north eastern casing stones, the mean opening of the joints is only 0.5 mm wide (1/50th of an inch). There are three known chambers inside the Great Pyramid as follows: (a) The lowest chamber is cut into the bedrock upon which the pyramid was built and was unfinished. (b) The so-called Queen's Chamber and King's Chamber are higher up within the pyramid structure. The Great Pyramid of Khufu at Giza is the only pyramid in Egypt known to contain both ascending and descending passages. Originally, the Great Pyramid was provided with a stone cladding that formed a smooth outer surface; what is seen today is the underlying core structure. The cladding can still be seen around the top part of the Pyramid [4]. As shown in (Fig. 1a).

Pharaoh Chephren (Khafre), son of Khufu, built the second pyramid in Giza, around 2520 BC. His tomb also included the Sphinx, a mysterious limestone monument with the body of a lion and Pharaoh's head. The Sphinx may stand guard for the entire tomb of the Pharaoh, as shown in (Fig. 1b).

One-third of the pyramids of Giza are much smaller than the first two. Built by Pharaoh Mykerinos (Menkaure) around 2490 BC, the temple houses much more complex funerals. The Menkaure pyramid is built at the far end of the Giza diagonal on the edge of the Mokattam formation, where it dips down to the south and disappears into the younger Maadi formation. The complex includes a valley temple, a causeway, and a mortuary temple on the east side of the pyramid. The pyramid's base lies 2.5 m higher than Khafre's pyramid and occupies only a quarter of the area used by the Khafre and Khufu pyramids. With its original height of 66 m, Menkaure's pyramid represents only about a tenth of the mass in comparison to the Khufu pyramid [5]. The bottom-most 15 m of the pyramid were cased with granite blocks

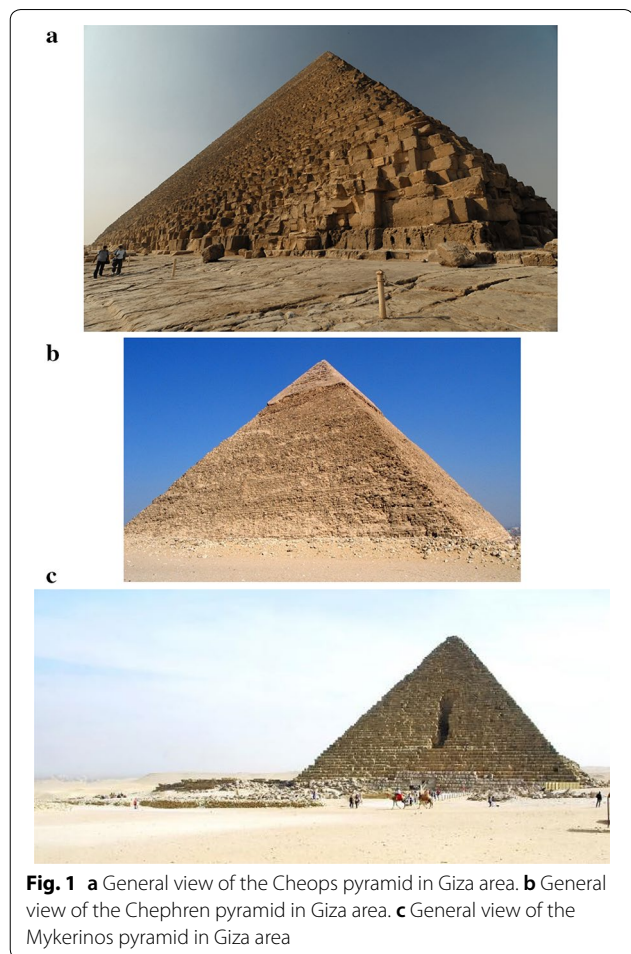


Fig. 1 a General view of the Cheops pyramid in Giza area. b General view of the Chephren pyramid in Giza area. c General view of the Mykerinos pyramid in Giza area

from Aswan. Further up, the casing was made of fine limestone.

Each huge pyramid is only one part of a larger complex, including palace, temples, solar boat pits, and other features, (see Fig. 1c).

The Giza plateau was in ancient times, geologically connected to the Moqattam hill on the other side of the Nile crossing the site of what is now the capital Cairo. The top level of the Moqattam hill is now + 200 m. The top level of the Giza plateau must have acquired a level hypothetically close to the Moqattam surface level, i.e. + 200 m, or so. The geological formation of both sites, the Giza plateau and the Moqattam hill, is composed of a cretaceous nucleolus amid an Iocenean formation, an action happened when Abu-Rawash concave cap mass was transposed upside down in the late upper cretaceous, resulting in a solid cap well exposed on the surface". Amid that process, the site was formed as hill heights along with convexes of the vallies, keeping an “axis running from the eastern North to the western South” [6]. That axis almost coincides with the axis connecting the

centers of gravity of the three pyramids. “The iocenean formation of the site is mainly composed of two strata, one higher and one lower. The lower stratum is identified as denser and more homogeneous.”

Conservation of historic buildings and archaeological sites is actually one of the most difficult challenges facing modern civilization. It involves a number of factors belonging to different areas (cultural, human, social, technical, economic and administrative), intertwined in inseparable patterns. The complexity of the topic is that it is difficult to imagine guidelines or recommendations that summarize what needs to be done and describe activities to continue, intervention techniques, design approaches.

From the point of view of the engineer, the specificity of this type of intervention is a requirement of respect for safety, along with ensuring safe use.

In the context of the principles of restoration, maintain the full integrity of The monument must be a well-accepted concept and this requires not rushing to stabilize measures until the monument’s behavior is properly understood.

Topography, geology, climate and human actions seem to have a significant impact on environmental processes, and therefore a significant impact on the conservation of the built environment.

The pyramid complex suffered from different types of structural damage and construction materials decay and disintegration. The sources of this degradation can generally be classified as: nature, time, and man-made. In recent years, the great pyramids and the Great Sphinx have been threatened by rising groundwater levels caused by water infiltration from the suburbs, irrigation canals and mass urbanization surrounding the Giza plateau [7]. The rising of groundwater levels represents a threat to the Egyptian Heritage of the Giza Pyramids Plateau (GPP) particularly since the area surrounding the plateau has been developed into the suburb of Greater Cairo. Today, Giza is a rapidly growing region of Cairo. Population growth in Egypt continues to soar, leading to new construction. New roads for large new developments are increasing obviously in the desert hills northwest and southwest of the Giza pyramids, As shown in space station views in (Fig. 2a–d).

Understanding the passage ways of rain water on the plateau, groundwater and sewage from both the Nile flood plain and Abo Roash area play an important role in the conservation strategy for the unique artifacts of the Giza Plateau Two regional aquifers are located behind the Sphinx statue with a water level at a depth of 1.5 to 4 m below the surface (for example). The second aquifer is a broken carbon aquifer that covers an area beneath the pyramid and sphinx plateau, where the depth of the

groundwater ranges from 4 to 7 m. The recharge of the aquifer underneath the Sphinx area occurred mainly through diversion of the water network and overall urbanization [7].

Due to the unique values of the three great pyramids in Giza, the present work is very important to analyze the nature and sustainability of the construction materials of the pyramid complex also to assess the effects of mechanical, dynamic and physiochemical actions of deterioration and structural deficiency, especially earthquakes and weathering impact on the pyramid structure.

Materials and methodology

Several tests and laboratory analyzes were carried out to determine the problems of the nature and sustainability of the outer casing stone blocks (granite, marble and limestone), filling stone blocks (limestone) and the structural mortars joining the stone units used in the construction of the three great pyramids in Giza. To investigate the above questions, we selected a total of 45 samples of fallen fragments from different locations around the three pyramids. The selected samples belong to the back layers and facades and represent typical building material features.

The laboratory work was carried out on site:

- Photographic documents, architectural and geodetic survey of the pyramid.
- Geomorphology, petrographic and chemical analysis.
- Engineering properties and mechanical analysis of stones and structural mortars.
- Record all cracks.

Eight thin sections were examined using polarized light microscopy to identify the petrographic and geochemical characteristics of these building materials (stones and binding mortars). X-ray diffraction (XRD) and X-ray fluorescence (XRF) probes were conducted to identify slices and ratios of the installation stones and mortar. Together with Scanning electron microscopy (SEM) attached with Energy dispersive X-ray (EDX) for microscopic examination and microscopic examination. Examples of XRD diffraction for both studied stones and slurry tests are increased by Cu K. radiation. The filtering speed is $2\theta = 1^\circ/\text{min}$. With a constant voltage of 40 kV, 30 m and the use of X-ray diffraction PW 1480. Significant components (by weight %) of stone and mortar tests studied using X-ray fluorescence spectrometer (XRF) were performed on an advanced wavelength-dispersed spectrometer (Axios, WD- XRF Spectrometer, PANalytical, 2005, Netherlands). The chemical analyses were carried out adopting the ASTM specifications (ASTM C114-00, (ASTM C114-15)”), and electron microscopy images

Fig. 2 **a** Space station view, photograph taken by astronauts in (2001, August 15). Roads and new constructions for large new developments are obvious in the desert hills northwest and southwest of the Giza pyramids. After NASA-JSC Gateway to Astronaut Photography of Earth (<http://eol/jsc.nasa.gov/sseop>). **b** Space station view, photograph taken by astronauts in (2012, August 18). The new constructions in the desert hills northwest and southwest of the Giza pyramids rapidly increased. After NASA-JSC Gateway to Astronaut Photography of Earth (<http://eol/jsc.nasa.gov/sseop>). **c** Space station view, photograph taken by astronauts in (2016, May 3). The new constructions in the desert hills northwest and southwest of the Giza pyramids extended many times. After NASA-JSC Gateway to Astronaut Photography of Earth (<http://eol/jsc.nasa.gov/sseop>). **d** Space station view, photograph taken by astronauts in (2019, October 14). The new constructions in the desert hills northwest and southwest of the Giza pyramids. After MAXAR Technologies 2019 (<https://eol.jsc.nasa.gov/>)

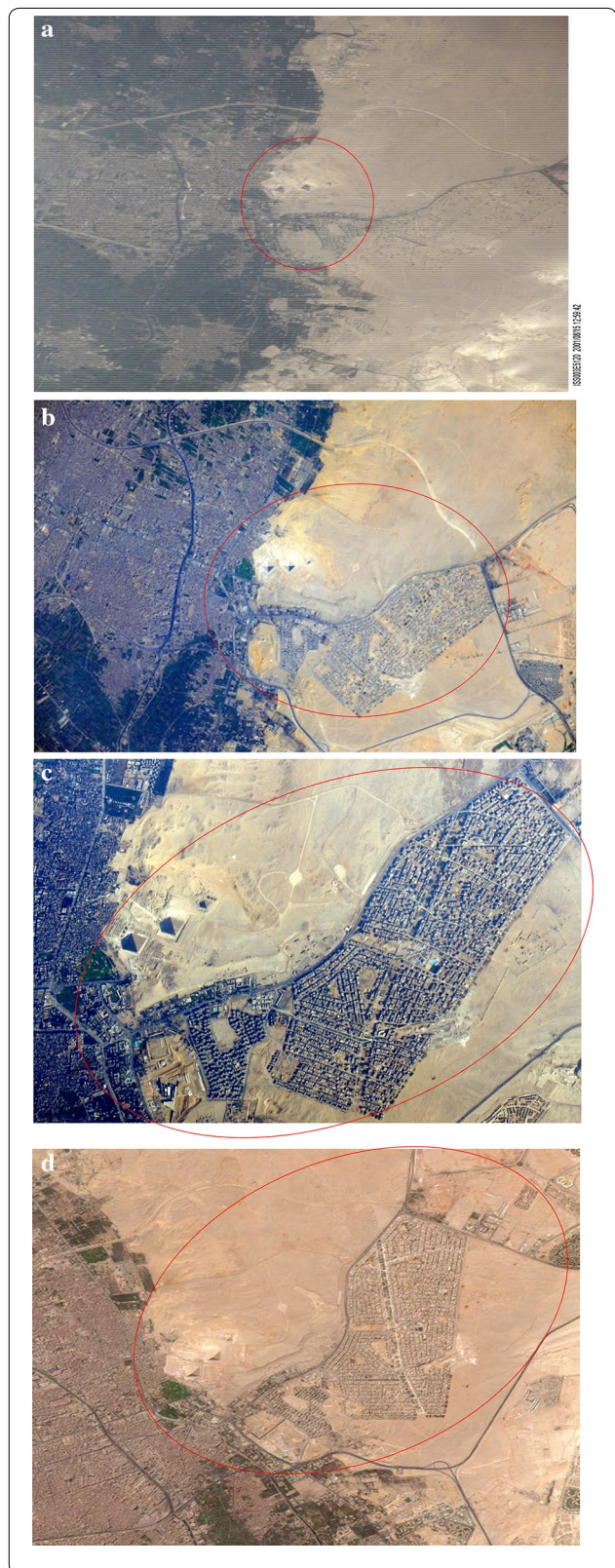
(SEM) were performed on a smaller scale analyzer JXA 840A for electron testing, Japan,

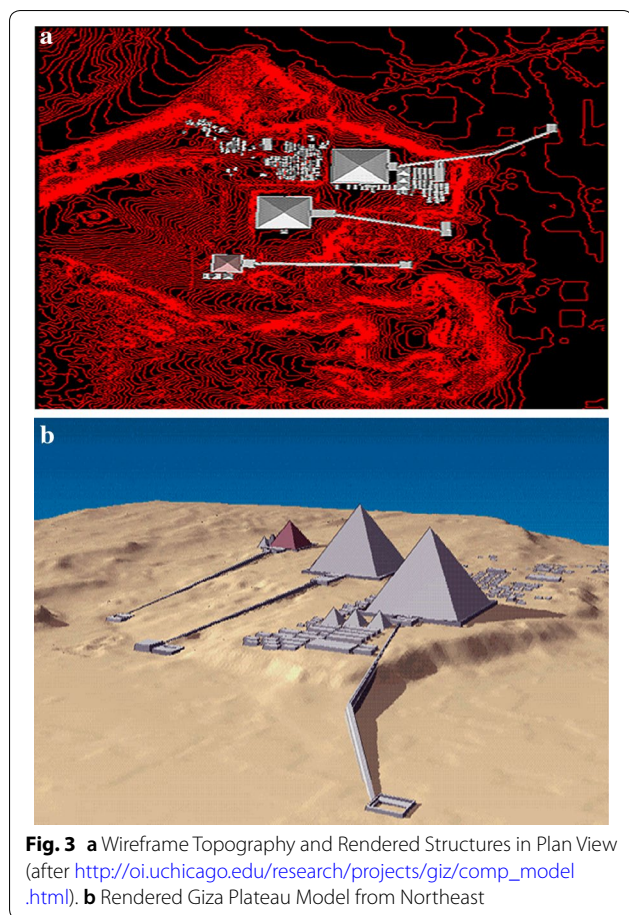
Engineering characteristics of the studied building materials (granite, limestone and structural mortar) were achieved. Fifteen cylindrical samples of stones were prepared to determine the petrophysical and geochemical properties. Specific gravity (G_s), unit weight (γ), water absorption (w_c), porosity (n) and saturation (s_r) are the specific physical aspects. While the mechanical characterization included the determination of uniaxial compressive strength (σ_c), Young's modulus (E) and Brazilian split tensile strength (σ_t), shear strength (T), Schmidt hammer index recovery number (SHV), durability or impact indexes are estimated by AIV, in addition to the non-destructive pulse ultrasonic wave velocity test (V_p) through stone examples, estimates of Young's dynamic coefficient (E_d) and shear modulus (G) [8].

Geomorphologically and geological context of Giza plateau

The Cheops, Khephren and Mykerinos pyramids are located in the north-western part of the Giza plateau (see Fig. 2). The altitude above sea level of the rock bases surrounding these monuments is approximately 68 m for Khephren and 62 m for Kheops (60 m at the SE corner), as shown in (Fig. 3a, b). The Sphinx and Queen Kentkawes' Mastaba lie further down on the plateau towards the Nile Valley. Their rock base altitudes are approximately 22 m around the Sphinx and 38 m around Kentkawes [9].

Geomorphologically, the area under consideration is divided into four distinct units: the plateau, the cliff and the slopes, terraces and the Nile flood plain. The height of the plateau ranges from 20 m in the northeastern and eastern bottom and 105.8 m in the peaks of the Western side top summits [10]. The top of the Giza plateau is flat and varies in height from 60 to 106 masl whereas the elevation of the area of the pyramids vary from 60 to 70 masl. The dip





angles range from 4° to 7° for the eastern part of the plateau near the Sphinx [11].

The studies show that the monuments of the fourth dynasty of the plateau of Giza are built on a sedimentary sequence with dominant carbonated formations deposited in an epicontinental sea of variable depth. All the authors agree that these sedimentary layers have the characteristics of the Mokattam formation and Maadi formation, from Middle to Late Eocene age, as shown in (Fig. 4a–c).

OMara [12], Yehia [13] and El Aref and Refai [14] carried out structural studies on the Giza Pyramids Plateau. The plateau is an oriented NE–SW and dipping SE monocline. This monocline is the SE anticlinal limb of the Wadi El Toulon anticline, lying in the southern part of the Abu Rawash folded complex. The dip of the layers of this monocline structure is homogeneous. El Aref and Refai [14] gives a value ranging between 4 and 7° for the zone carrying the study sites.

This monocline is affected by hectometric faults with normal dominant and weak throw oriented NW–SE which does not affect the study sites. On the 1/100,000 map of Greater Cairo the plateau is located in the Mokattam formation of the Middle Eocene, linked in the south by faults

with the Maadi formation of the Late Eocene. The weak throw and the orientation of these faults essentially suggest a discrete deformation by synsedimentary normal faults during the Eocene deposition period.

The entire plateau is affected by karstic processes, described by El Aref and Refai [14] and Dowidar and Abd-Allah [11], which developed according to the local structural and stratigraphic conditions and led to a particular morphology of stepped terraced escarpments, karst ridges and isolated hills. These authors relate the development of karst features to Mediterranean climatic conditions [9].

From the observations made in the boat-pits, at the NE corner of the Cheops pyramid and on the esplanade around the pyramid, we have seen that the rock base of the monument is mainly composed of nummulitic packstone.

Observations at Cheops' pyramid show that the rocky basement is not very visible in the lower parts of the pyramid. It is however possible to establish the presence of original rocky hill, as shown in (Fig. 5a, b). The Northern East corner of the great pyramid of Khufu is the visible part of the original hill [9].

Petri [15] observed the rock in the inner proportions at an altitude of 8 m above the level of the scheme. For Eyth [16] the maximum height of the rock platform is 12.5 m, and Dormion [17] is only 6.60 m. They observed natural rock in the galleries of the pyramid of Cheops and Khephren where the lining of the walls had disappeared [9].

The study area fractures are found in three major groups heading west–northwest, northwest and north–east. Fractures to the west and northwest are predominant in the northern, western and eastern sides of the Pyramids of Cheops and North of the Pyramids of Khephren [9–11].

Depending on the depth of the 2012 groundwater contour map, there are two groundwater systems in the study area. The first part relates to the groundwater aquifer system and covers the eastern part of the Sphinx area where the depth of the groundwater ranges from 1.5 to 4 m below the surface of the ground and increases the depth of groundwater west. The second system is linked to water. The bearing layers belong to the formation of broken limestone (below Sphinx area), where the depth of groundwater ranges from 4 to 7 m below the surface [7].

Structural damage and materials decay

Dynamic actions

According to historical recordings the strong earthquakes and seismic events that have struck the Giza area induced small or medium damages and structural deficiency to

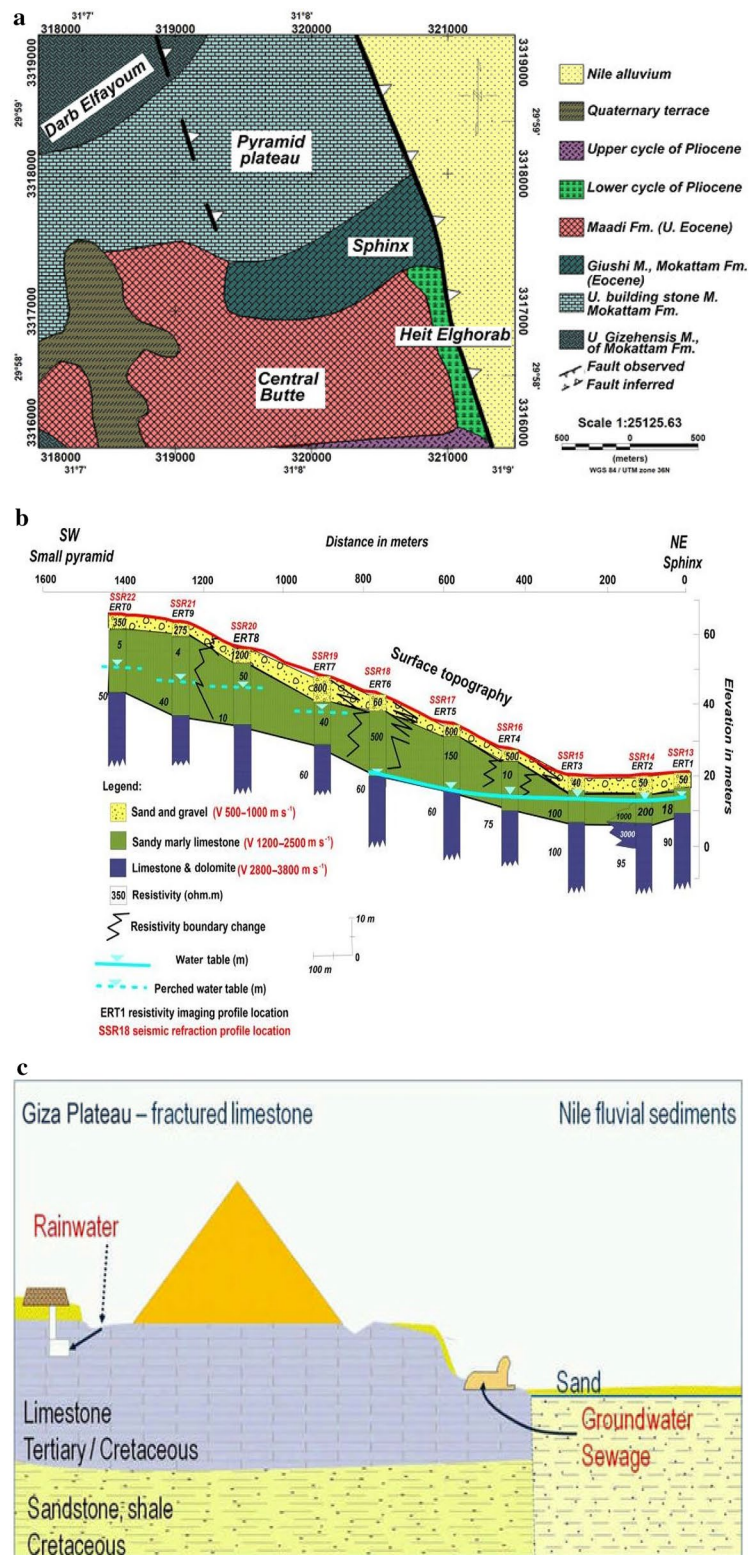


Fig. 4 **a** The geological setting of the Giza plateau, where the pyramids are built (modified after Yehia [12]). **b** A cross section using the ERT data shows how the groundwater elevation changes from the Sphinx to Menkaure Pyramid. It indicates an increase in groundwater elevation from west to east) (modified after Sharafeldin et al. [17]). **c** Groundwater aquifers affecting the Giza Plateau (modified after ElArabi et al. [30])

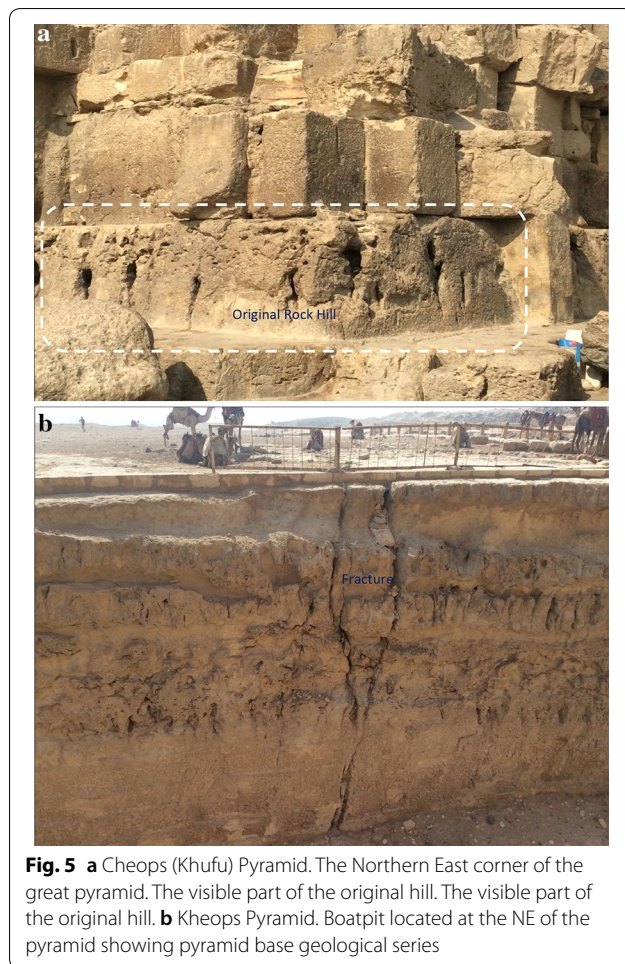


Fig. 5 **a** Cheops (Khufu) Pyramid. The Northern East corner of the great pyramid. The visible part of the original hill. The visible part of the original hill. **b** Kheops Pyramid. Boatpit located at the NE of the pyramid showing pyramid base geological series

the pyramids complex. Up to the end of the ninth century the secular number of reported earthquakes fluctuates between zero and three. A relatively high number (eight) of earthquakes has been reported in the tenth century. The reported earthquakes reach their highest number (17) in the nineteenth century [18].

The Question: What is the reason for the proven resistance of the monuments to the seismic events of the past? The good seismic behavior of the Giza plateau (limestone tertiary/cretaceous) or is it that the way in which the buildings were constructed enabled them to withstand successfully the seismic actions.

The instrumental seismicity map indicates that the pyramids site is characterized by very low seismicity setting [19].

The site selection and the geological properties of the area, being away from seismic effects, floods and groundwater levels, the stability of the geometric form of the pyramid, the solidity of the structural engineering and precision of execution arguably are the reasons why the Great Pyramids of Giza are the only survivors of the seven

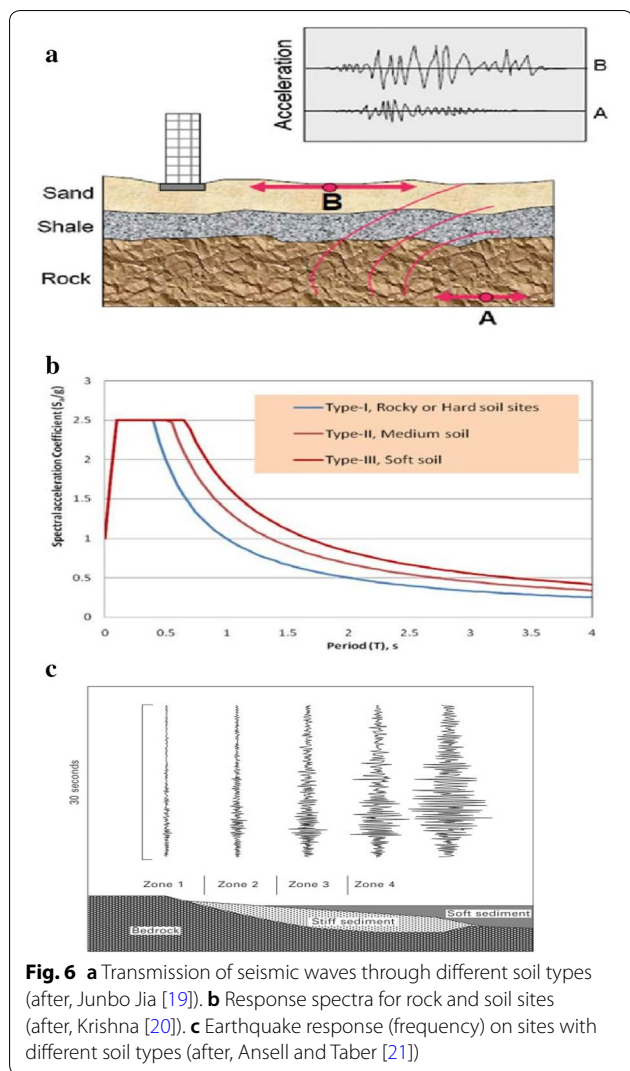
wonders of the ancient world. Most of the destructive earthquakes' epicenters are localized in the eastern bank of the River Nile. Also, the isoseismal intensity contour map reflected that the pyramid site has not been affected by intensity value more than VI on Mercalli scale. Moreover, one of three seismotectonic trends affecting Egypt passes by Fayoum province but avoid the Pyramids' site.

The sedimentary layers where the pyramids were considered a suitable foundation that can safely support the massive rock structure.

The good seismic behavior of the Giza plateau (limestone tertiary/cretaceous Formations) is a result of the transmission of the earthquake acceleration in the limestone or rock Formations is much lower than the transmission of the same earthquake acceleration in the soft and medium soils, as shown in (Fig. 6a) [20]. Also the spectrum acceleration coefficient and force in the rock Formations are much lower than the spectrum acceleration Coefficient and larger force in the soft and medium soils in particular the clay soil as shown in (Fig. 6b) [21]. Note: soil type coefficient should be examined for the top 30 m of soil or rock Formations layer. Also the ground accelerations are strongly modified by the soil conditions. Rock sites will have high frequency shaking, while on soft soil sites high frequencies (short period) will be reduced or filtered out, but low frequencies will be amplified as shown in (Fig. 6c) [22].

The construction details, where the rock keys were used to stabilize the slope against slippage in the Great Pyramid (very functional especially during earthquakes). It is amazing to note that the maximum static stress under the Greater Pyramids is about 3500 kPa; yet this huge stress value did not entail any observed or likely foundation failure (bearing capacity or excessive settlement). Show that the builders had taken into consideration the likelihood of seismic loading. Founding of the monuments for the most part on solid rock and good quality of construction of the foundations favour their good anti seismic behavior.

The Pyramidal shape represents an extraordinary advantage, since the pyramid is the most earthquake-resistant structure possible, even more than the domes. For the construction details; several layers of smoothed stones without any mortars or sticky materials between them actually form a kind of base isolation for the foundations, where some flat small stones like pillow were laid to absorb the first shock of earthquake force on the pre-prepared soil under foundations. Some big stones layers were put over these small stones. The number of layers in most of the times was three and no mortar was used, the large foundation stones are called "Orthostat" stones. The pyramid shaped building is suitable in



earthquake prone area due to its higher stiffness and less displacement.

The only earthquake that affected the pyramids was in the 14th century on August 8, 1303. A massive earthquake ($M=6.5$ Richter) hit the Fayoum area and loosened many of the outer casing stones, some of the stones can still be seen as parts of these structures to this day. Later, explorers reported massive piles of rubble at the base of the pyramids left over from the continuing collapse of the casing stones which were subsequently cleared away during continuing excavations of the site. Nevertheless, many of the outer casing stones around the base of the Khufu Pyramid can be seen today in site, displaying the same workmanship and precision as has been reported for centuries [19]. Table 1 represents the Earthquakes causing intensities VII or greater near Giza area.

In August 1303 AD, Eastern Mediterranean: A strong shock was felt throughout northern Egypt. Arabic sources reported that this earthquake was the strongest in Egypt, particularly in Alexandria. In Cairo, almost all houses suffered some damage and many large public buildings collapsed. The earthquake caused panic, and women run into the streets without their veils. Minarets of the mosques of Cairo were particularly affected. In Alexandria, many houses were ruined and killed a number of peoples. The lighthouse was shattered and its top collapsed. The damage extended to Southern Egypt up to Qus. This earthquake was placed by Sieberg to Faiyum, south of Cairo because of the severe damage in Middle Egypt. It was also reported that this earthquake caused large-scale damage in Rhodes and Crete. Ambraseys [23] placed its epicenter in the Mediterranean Sea as As-Souty mentioned that the advance of sea submerged half of Alexandria. According to Arabic sources (e.g. El-Maqrizy; As-Souty) aftershocks continued during 3 weeks [18].

Recently the present area is near to relatively active earthquake area to the west of downtown Cairo. In that area, the most destructive event in recent history of Egypt took place in October 12th, 1992. The epicentral distance is only about 30 km. Damage report after that earthquake showed that great pyramids at Giza were severely damaged, and few years later a restoration plan was inaugurated to save the pyramids from more damage and instability problems. In addition, other earthquake activities are also observed at east Cairo, like Aqaba earthquake in 1995. But Dahshour seismic zone constitutes the epicenter of the 12th October 1992 Cairo earthquake, and other seismic activity area produced earthquakes with magnitudes seldom reaching a magnitude of 5. However, due to their proximity from the dense population Cairo metropolitan, such earthquakes were widely felt in greater Cairo area. The seismic zone at Dahshour is only few kilometers from the pyramids complex. The epicentral distance between Cairo earthquake and pyramids is few kilometers only. This proximity indicates that Dahshour seismic zone might have the highest effect especially at short periods.

Most of the typical land failure effects were as extensive as soil liquefaction [24]. Giza Governorate was exposed to liquids during the 12 October earthquake [25].

Soil liquefaction has been reported in Giza. Since this is the last major earthquake affecting the monument, it is possible to assume that the present deformed form and the cracking of the inner chambers and the inner and outer stone layers [26–29]. According to the Egyptian newspaper Al-Ahram in 13 October 1992, several small outer casing blocks on the top of the great pyramid and

Table 1 Earthquakes causing intensities VII or greater near Giza area. Modified after Kebeasy et al. [27] and Sykora et al. [28]

Date	Location of epicenter	Epicentral intensity	Cairo (locational) intensity	Remarks
2200 BC	Tall Basata	VI	–	M = 5.8. Deep fissures and soil cracks in Tall Basata
24–20 BC	Alex offshore	–	–	Strong sea waves
320	Alex offshore	VII	VII	Many houses destructed
796	SE Mediterranean Sea	VI	–	Felt at different localities of Egypt, partial damage of Alex Light House
5/26/1111	East Cairo	VII	VII	Destruction of Rehachope Temple
8/8/1303	Fayum	VIII	VI	M = 6.5. Severe earthquake: many places in Cairo were destructed, affected the Nile Valley till Quoos and little damage
1326	Alex offshore	V	–	Light house was shocked, felt in many places
1687	Alex offshore	VI	VI	Alexandria was vibrating for 10–12 days
9/1754	Tanta	VIII	VII	Two-thirds of Cairo buildings damaged. 40,000 fatalities'
8/7/1847	Fayum	VIII	VI	3000 houses and 42 mosques destroyed. 85 fatalities
1870	East of Mediterranean	X	–	M = 7. Severe earthquake, felt in vast area 32° N, 30° E
1908	Alex offshore	–	–	Strongly felt earthquake
10/1/1920	29.4° N 31.0° E	VII	V-VI	M = 5.8
10/12/1992	29.89° N 31.22° E Dahshuor	VIII	VII	Ms = 5.2 HL, = 5.9 Mo = 8×10^{17} N-m Depth 25 km

supporting panels fell down during the Dahshuor earthquake 1992.

It is important to note that after the first earthquake, permanent distortions (and therefore moments of permanent curvature) remain, so that global behavior, even in the case of low-level earthquakes, becomes weaker and weaker. The structure is weakened after earthquakes between the blocks and deformations of the exits and pressure in the walls; from this point of view, the current situation is worse than in the past, as shown in (Fig. 7a, b). Permanent deformation of blocks in the zone of borders of the façades and corners of the great Cheops' pyramid. The increasing weakness of the structure after earthquake causing the friction and sliding between the casings and filling blocks. Show extremely slow degradation process which affected the backing stone blocks of the great pyramid, many blocks were detached. The outer casing stone blocks fell down completely in 1303 strong earthquake.

After the 1992 earthquake, the Giza pyramids remained deserted and thus suffered a gradual deterioration. Attention initially focused on the lateral boundaries of the remaining facades, where discontinuity and consequently the disappearance of peripheral stress led to a very disadvantageous situation, exacerbated by the dynamics that affected the current boundaries of the areas at risk.

The walls of the pyramid complex suffered from shear forces due to previous earthquakes; vertical cracks and

cracks with a direction of about 35–45° above the horizontal, shows the corresponding failure mechanism. Some cracks affect specific elements such as thresholds for openings, doors and foundation stones, as shown in (Fig. 8a, b). Cracking of backing limestone blocks due to the overloading and material decay and strength regression, which affected the great pyramid stability. The honey comb (differential) weathering aspects are obvious on the surfaces of backing limestone blocks. The outer facing limestone blocks are missed completely.

It is difficult to determine the actual degree of stability. Despite this uncertainty, the state of internal pressure of the structure, on the contrary, is well defined. Loss of balance cannot occur during the adjustment. This is the correct aspect of the behavior of building structures that can explain the great durability and longevity of many historic buildings.

The old builders were not Civil engineers. While the modern engineer's interest is to prevent settlements, the old engineers were willing to allow the movements of institutions and the resulting cracks. There is something unique in the behavior of construction structures. This is due to the mechanical construction response, and differs significantly from those shown by the usual flexible materials. The difference is due to the low tensile strength of the construction and to the different response of the construction in stresses [30]. The pyramids were severely damaged on the surface of lower-level stone walls due to

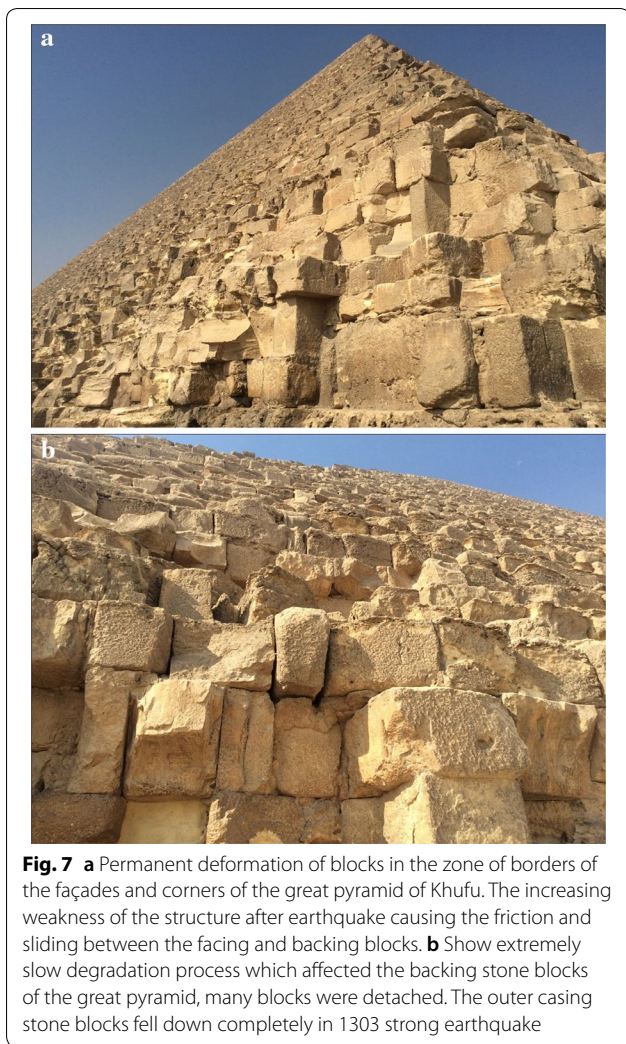


Fig. 7 **a** Permanent deformation of blocks in the zone of borders of the façades and corners of the great pyramid of Khufu. The increasing weakness of the structure after earthquake causing the friction and sliding between the facing and backing blocks. **b** Show extremely slow degradation process which affected the backing stone blocks of the great pyramid, many blocks were detached. The outer casing stone blocks fell down completely in 1303 strong earthquake

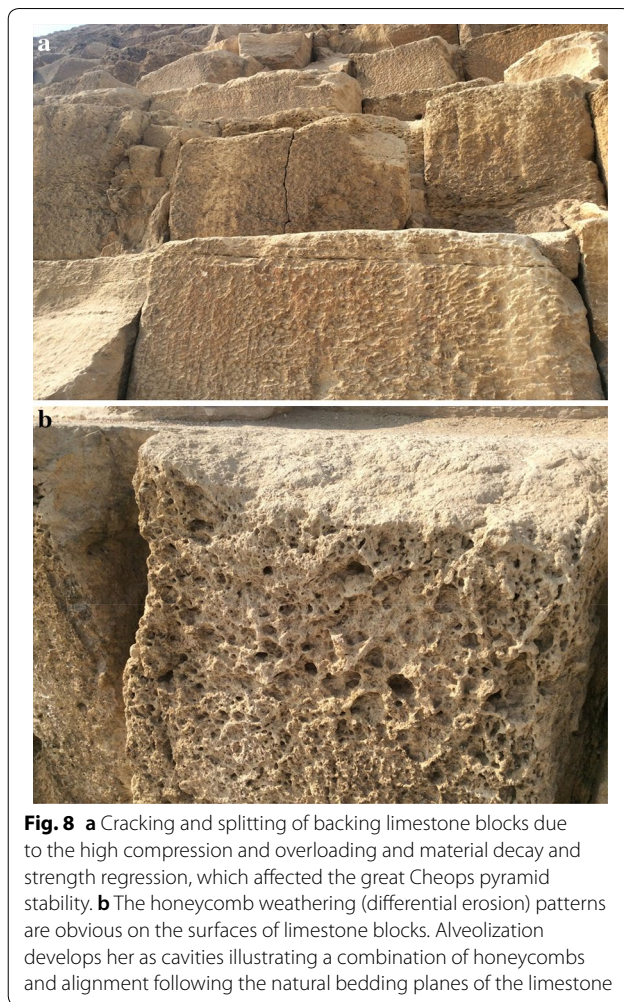


Fig. 8 **a** Cracking and splitting of backing limestone blocks due to the high compression and overloading and material decay and strength regression, which affected the great Cheops pyramid stability. **b** The honeycomb weathering (differential erosion) patterns are obvious on the surfaces of limestone blocks. Alveolization develops here as cavities illustrating a combination of honeycombs and alignment following the natural bedding planes of the limestone

long-term static and dynamic actions, extensive cracks in walls caused mainly by settlements, and only because of seismic loads while the foundation stone sites were specifically removed.

Physiochemical actions

The climatic conditions in the study area are semi-arid; warm in winter with little rain and hot to dry in summer. The climate is characterized by the following parameters. With regard to precipitation, the average annual rainfall does not exceed 25 mm, which is generally rare throughout the year, sometimes occurring in the form of sudden and short showers associated with wind. The average annual relative humidity is around 46% with a maximum of 70% in November and a minimum of 30% in May. The maximum annual temperature is 28 °C while the lowest annual temperature is 13.8 °C. For winds, the prevailing wind blows are from the northwest and the monsoon

known as Khamasin from the southwest and south. Wind speeds range from 7 to 14 km/h [31].

The great pyramids at Giza and have been threatened by rising groundwater levels caused by water infiltration from the suburbs. Irrigation canals, mass urbanization surrounding GPP, (as shown in Fig. 2a–c). Two regional aquifers are located behind the Sphinx statue with a water level at a depth of 1.5 to 4 m below the surface (for example). The second aquifer is a broken carbon aquifer that covers an area beneath the pyramid and sphinx plateau, where the depth of the groundwater ranges from 4 to 7 m. The recharge of the aquifer underneath the Sphinx area occurred mainly through diversion of the water network and overall urbanization. The shallow water table elevation at Nazlet El-Samman village reaches 16–17 m and might recharge the aquifer below the Sphinx and Valley Temple, which is considered a severe hazard on the site [7].

There is deterioration in many parts of the three pyramids, associated with the aging of materials and the

impact of aerial and ground water attack, and extreme stresses and cracks have accelerated the related phenomena, as shown in (Fig. 9a, b), extremely slow degradation process which affected the backing limestone blocks of the Cheops, Chephren and Mykerinos pyramids is obvious. Many blocks was detached and are hanging.

The pyramid stones are characterized by minute cracks, thin and superficial fractures, gaps in the stone veneer, separate stone layers and large gaps below the surficial hard crust.

The backing limestone of the three pyramids are characterized by deep and hollow pits on the surface crust. They are very thin and are based only on a few points. Some parts have lost their shell, and for this reason, large parts are characterized by strong separation. A severe phenomenon is the separation and peeling of the limestone layer due to the capillary rising of ground water, as shown in (Fig. 8).

The backing limestone blocks characterized by weak cementation and adhesion due to the presence of small cracks, or pores, of secondary origin resulting from salt weathering.

Our analysis showed that the poor state of conservation of the three pyramids can be attributed to two main factors: internal (or intrinsic) causes, related to the characteristics of the fossil limestone itself (e.g., mineral composition, stratification, fractures, etc.) and external causes (or Externalities), due to external factors (such as ground water, climate change etc.). While the latter began the process of weathering on limestone blocks, the development and increase of this process is due to lack of cohesion in limestone cement. In fact, the very poor state of maintaining interior walls is due to several internal factors, as in the past, are strictly interconnected.

On the other hand, external causes are associated with daily-acute environmental factors Seasonal thermal changes, solar radiation, wind direction and density—work in synergy with the internal causes of limestone degradation.

The most obvious and most common phenomenon is peeling (or lids) due to the capillary rising of ground water, specific both on the surface, in the form of high elevated chips, deeper parts, with thick detachable layers of limestone blocks. The layer is associated with temperature changes that cause the expansion and contraction cycles of the material, resulting in strong mechanical pressures.

Cracking within crystals is also very common in the fragile deformation of posterior limestone blocks characterized by high gaps. Means within crystals (not between) crystals. In highly penetrating stones, pressure builds up through the grain—the grain contact becomes large



Fig. 9 **a** Show the limestone chipping under high compression and loading. Also represents the extremely slow degradation process which affected the backing limestone blocks of the Mykerinos, pyramid. Many blocks was detached and are hanging. **b** The outer casing granite blocks fell down completely due to the 1303 strong earthquake. The scattering of the granite facing blocks around the pyramid area is obvious

because the forces spread over very small areas (stress is the strength of each area), making it easily breakable internally than if porosity is small or non-existent.

The degradation of granite blocks casing the Mykerinos, pyramid is a complex process resulting from the interaction of many associated factors such as climate zone, a rising groundwater table resulting from water leakage from the suburbs irrigation canals, and mass urbanization surrounding the Giza pyramids and material properties that ultimately lead to chemical, physical/mechanical and biological weathering. Moreover, the behavior of building materials under weathering conditions is predicted by the design of the element and constructive elements. On the other hand, there are some specific weathering forms that affect different granite blocks depending on the surrounding environmental conditions such as red crusts that dominate the case study of aggressive alternative drying and urination cycles, as well as other chemically or biologically related

degradation factors for the weathering rates of silicate minerals. Thus, it can be emphasized that the particular weathering model that characterizes our effects is due to all these factors and associated mechanisms; they consist mainly of complex types of iron oxide-dyed clay minerals. All these factors above require some conservation measures to protect the monuments through various scientific strategic plans containing many preventive and multiple measures.

Human impact

The pyramids used to be cased. The great Cheops pyramid was covered with outer casing white fine limestone blocks from Tura limestone quarry, only a few of these now remain at the pyramid's base on the corners. The backing limestone blocks of Chephren pyramid was covered and cased with fine limestone blocks, also the stone cap now remain on the top of the Chephren pyramid. The Mykerinos pyramid was covered and cased with granite facing blocks were quarried and imported from Aswan quarry, 1000 km from Cairo.

During the middle Ages, much of the pyramid's outer facing blocks were fell sown because of the 1303 earthquake, Table 1. Many facing blocks were taken and reused for the buildings of many Coptic and Islamic monuments in Cairo city, revealing the Fossiliferous limestone backing blocks.

Construction of the pyramids of Giza

The fact now that the surface level of the area to the west of Cheops pyramid reaches + 110 m does not mean that it was the original height before its construction, as shown in (Fig. 3). Moreover as up mentioned, the other part of the formation—the Moqattam—on the east of the Nile is having an elevation + 200 m. Having this fact, and investigating the formation of the stones of the building material of the pyramid and the ground surface where pyramids were built, one could easily find that the former one was chosen from the upper stratum of Eocene site while the latter one is the original lower dense stratum of the Eocene which was used as a base for the structure, as shown in (Fig. 4a).

In the mean time, to have the three pyramids visually well perceived from Iunu, their bases' levels acquired 10 m difference from each other i.e. Khufu's was on + 60 m, Khafre's on + 70 m, and Menkaure's on + 80 m. By mentioning that, the sum of masses of the pyramids almost reached 13.5 million tons, it should be said that as this was the dynamic weight, the equivalent static weight in place prior to the construction was five or six times, i.e. 67.5 or 81 million tons. That was the net weight of the blocks but, if we consider the wasted rubble resulted from shaping the blocks that number could easily have been doubled i.e.

around 160 million tons. If the plateau was considered as the area between the contour lines of + 60 and + 80, then the area was 797,692.5 m². That means that the height of that area could have reached level + 160 m or higher. So, that height was used as the building material in situ for the pyramid. Having that elevation of the original plateau, the logic tells the fact of transposing the huge masses extracted from the high levels to levels below, and eight ramps were used to roll blocks down. There is an example of such a ramp in front of the second pyramid [32].

It is noticed that the Great Pyramid was built on a carved outcrop using the existing topography at the time of its construction. The part of original hill constitutes 23% of the volume for the Khufu/Cheops Pyramid and the carved outcrop constitutes 11.5% of Khafre Pyramid [19].

Results and discussion of the petrographical study

From the observations made in the digging of boats, in the northeast corner of the pyramid of Khufu and on the deck around the pyramid, we have seen that the rocky base of the monument consists primarily of nummulitic packstone. Observations in Kheops, pyramid, based on the same criteria as Khephren's pyramid, indicate that the rocky basement is very invisible in the lower parts of the pyramid. However, it is possible to prove the existence of an original rocky hill.

Mineralogical characteristics (by X-Ray diffraction)

X-ray diffraction was also used to identify minerals for whole stone powders and clay part. Semi-quantitative data are given for each metal present by their relative density the metal composition was determined by X-ray diffraction analysis, which was conducted through the National Center for Housing and Building Research in Cairo. Graphs of the representative body of limestone, specimens of structural limestone layers and samples of structural mortar layers were recorded. All results are summarized in Tables 2, 3, 4, 5, 6, 7, 8, 9.

The outer casing limestone blocks (Cheops's great pyramid)

The outer casing limestone consists of a whitish to whitish-yellow, very fine-grained limestone and can be easily distinguished from the heterogeneous filling limestone blocks with its much coarser microstructure.

Many of the outer casing stones and inner chamber blocks of the Great Pyramid were fit together with extremely high precision. Based on measurements taken on the north eastern casing stones, the mean opening of the joints is only 0.5 mm wide (1/50th of an inch).

Table 2 XRD analysis results of the casing fine limestone blocks samples of Cheops pyramid

Ref. code	Mineral name	Chemical formula	Semi quant [%]
01-072-4582	Calcite	CaCO ₃	100

Table 3 XRD analysis results of backing limestone blocks samples of Cheops pyramid

Ref. code	Mineral name	Chemical formula
01-072-4582	Calcite	CaCO ₃
01-074-3485	Quartz	SiO ₂
00-036-0426	Dolomite	CaMg(CO ₃) ₂
00-002-0818	Halite	NaCl

Table 4 XRD analysis results of structural mortars samples of Cheops pyramid

Ref. code	Mineral name	Chemical formula
01-072-0596	Gypsum	Ca(SO ₄)(H ₂ O) ₂
01-072-4582	Calcite	CaCO ₃
01-074-3485	Quartz	SiO ₂
01-071-4892	Dolomite	CaMg(CO ₃) ₂
01-072-0503	Anhydrite	Ca(SO ₄)

Tura limestone formations were used as coated casing stones to cover the local limestone filling blocks of the Great Pyramid of Khufu. Although some of the casing remains, most have been removed. However, each of the ten stones discovered had inscriptions on the back sides.

The outer casing limestone blocks are constructed from large white fine limestone with a mineral content of 100% calcite (CaCO₃), few blocks are still in place, mostly at the base. It may be extracted from Tura quarry that belongs to the Mokattam Plateau. Hair and cracks are filled with fine stone with dust and soft sand. The upper units are indicated by weak limestone blocks with structural mortars. The outer layers of casing or lumps are made of limestone, which is characterized by pure fine limestone, mainly from calcite CaCO₃ (100%) and the results of the analysis are shown in Table 2.

The backing limestone blocks (Cheops great pyramid)

The layers of backing limestone blocks which is irregular in size can be observed, these layers constitutes up to four courses lie between the outer casing layers and the core masonry, this core is not exposed.

The backing limestone blocks of Cheops great pyramid is composed mainly of calcite (CaCO₃) as the essential

Table 5 XRD analysis results of backing limestone blocks samples of Chephren pyramid

Ref. code	Mineral name	Chemical formula
01-072-4582	Calcite	CaCO ₃
01-074-3485	Quartz	SiO ₂

Table 6 XRD analysis results of structural mortars samples of Chephren pyramid

Ref. code	Mineral name	Chemical formula
01-072-0596	Gypsum	Ca(SO ₄)(H ₂ O) ₂
00-001-0994	Halite	NaCl
01-074-2421	Anhydrite	Ca(SO ₄)
01-085-1108	Calcite	CaCO ₃
01-074-3485	Quartz	SiO ₂

Table 7 XRD analysis results of the outer casing granite blocks samples of Mykerinos pyramid

Ref. code	Mineral name	Chemical formula
01-070-2537	Quartz low	SiO ₂
01-078-1995	Albite	Na(AlSi ₃ O ₈)
01-078-1254		SiO ₂
01-083-1604	Microcline	KAlSi ₃ O ₈
01-072-2300	Kaolinite-1A	Al ₂ Si ₂ O ₅ (OH) ₄
00-004-0594	Actinolite	Ca-Mg-Fe ⁺² -SiO ₂ -OH
00-046-1409	Muscovite-2M1, vanadial barian	(K, Ba, Na) _{0.75} (Al, Mg, Cr, V) ₂ (Si, Al, V) ₄ O ₁₀ (OH, O) ₂

Table 8 XRD analysis results of the backing limestone blocks samples of Mykerinos pyramid

Ref. code	Mineral name	Chemical formula
01-072-4582	Calcite	Ca(CO ₃)
01-074-3485	Quartz, syn	SiO ₂
00-006-0046	Gypsum	CaSO ₄ ·2H ₂ O

Table 9 XRD analysis results of the structural mortars samples of Mykerinos pyramid

Ref. code	Mineral name	Chemical formula	Semi quant [%]
01-086-2335	Calcite, magnesian	(Mg _{0.064} Ca _{0.936})(CO ₃)	55
00-019-0237	Rancieite	(Ca, Mn) Mn ₄ O ₉ ·3H ₂ O	15
00-005-0583	Triplite	(Fe, Mn) ₂ FPO ₄	10
01-074-3485	Quartz, syn	SiO ₂	20

component associated with minor amount of iron oxides and quartz (SiO_2) and rare of dolomite ($\text{CaMg}(\text{CO}_3)_2$), opaque minerals and halite (NaCl). Results of XRD pattern are presented in Table 3.

The main quarry area, supplying the backing and core masonry of the Khufu pyramid, was situated some 500 m south of the pyramid's southern edge. The more eastern parts of this central quarry field were generally exploited by Khafre to gain core material for his pyramid.

The structural joining mortars (Cheops's great pyramid)

The structural mortar joining the backing limestone blocks composed of gypsum ($\text{Ca}(\text{SO}_4)(\text{H}_2\text{O})_2$), rock fragments (composed of calcite and dolomite ($\text{CaMg}(\text{CO}_3)_2$), biotite, muscovite and rare quartz grains cemented by very fine-grained matrix of gypsum, anhydrite (CaSO_4), calcite admixed with minor iron oxides. The analysis results are presented and summarized in Table 4.

The backing limestone blocks (Chephren's pyramid)

The backing limestone blocks of Chephren's pyramid is composed mainly of calcite (CaCO_3) as the essential component associated with rare amounts of iron oxides, microcrystalline quartz and opaque minerals. Results of XRD pattern are presented in Table 5.

The structural joining mortars (Chephren's pyramid)

The structural mortar joining the filling limestone blocks is composed of gypsum ($\text{Ca}(\text{SO}_4)(\text{H}_2\text{O})_2$), anhydrite and rock fragments (composed mainly of calcite) associated with minor amounts of quartz, biotite, iron oxides and opaques cemented by very fine-grained matrix of gypsum admixed with calcite, anhydrite, halite and iron oxides. The analysis results are presented in Table 6.

The outer casing granite blocks (Mykerinos's pyramid)

The outer casing granite blocks of the Mykerinos's pyramid is composed mainly of potash feldspar (microcline, orthoclase and perthite), quartz and plagioclase associated with considerable amounts of hornblende and biotite and accessory amount of muscovite ($(\text{K}, \text{Ba}, \text{Na})_{0.75}(\text{Al}, \text{Mg}, \text{Cr}, \text{V})_2(\text{Si}, \text{Al}, \text{V})_4\text{O}_{10}(\text{OH}, \text{O})_2$), titanite, zircon and opaque minerals. Secondary minerals are represented by iron oxides sericite and clay minerals. The analysis results are presented in Table 7.

The backing limestone blocks (Mykerinos, pyramid)

The backing limestone blocks of Mykerinos, pyramid is composed mainly of calcite (CaCO_3) as the essential component associated with minor amount of iron oxides and rare amounts of quartz, gypsum and opaque minerals. Results of XRD pattern are presented in Table 8.

The structural joining mortars (Mykerinos, pyramid)

In the present study more than 6 mortars samples were analyzed in terms of determination of chemical composition and salt content. In an effort to correlate the salt content with the role and structure of the structural joining mortars.

The structural mortar joining the backing limestone blocks is lime based mortar and composed mainly of Calcite, magnesian ($\text{Mg}_{0.064}\text{Ca}_{0.936}(\text{CO}_3)$) (55%), Rancieite ($\text{Ca}, \text{Mn})\text{Mn}_4\text{O}_9.3\text{H}_2\text{O}$ (15%), Triplite ($\text{Fe}, \text{Mn})_2\text{FPO}_4$ (10%), Quartz, syn SiO_2 (20%). The analysis results are presented in Table 9.

Morphological description and qualitative microanalysis by SEM attached with EDAX

Microscopic examination and initial partial analysis on the front and back stone blocks and structural slurry samples from the three great pyramids were performed by the SEM attached with EDAX to study the texture, cement texture, fine image pores and the remaining carbonate portion on the filter paper to also identify structural mortar elements.

The backing limestone blocks from the three pyramids

The morphological investigation indicate that the Fossiliferous limestone (Biomicroite) bodies from the three pyramids contain different surface features, such as the wide distribution deteriorated crusts, corroded quartz grains and the presence of some large voids and micro pores, as well as, some disintegration aspects in each grain, as shown in (Fig. 10a, c d) for the filling limestone blocks from Cheops's pyramid (Fig. 15a, c) for the filling limestone blocks from Chephren, pyramid (Fig. 11a) for the filling limestone blocks from Mykerinos, pyramid.

The micro analysis with EDX for the filling limestone from the three pyramids complex revealed that the limestone consist mainly of specific elements such as (Ca, Si, O, Al, Ca, O, K, Na, Al, C), (Figs. 10b, 11b, and 13b).

The structural mortars from the three pyramids

SEM observations indicated that there is a relative deposition of calcium from the binder due to physical and chemical actions that reduced alkalinity and strength and increased absorption of this lime mortars. The lime linker becomes less hydraulic but has the highest resistance to perfusion, and some observations have indicated the presence of a condensed halite within the mortar composition. The presence of carbon and organic residues within the mortar composition was also apparent, as shown in (Figs. 12a, c, 13a, c).

Fig. 10 **a** SEM micrographs of limestone from the backing stone blocks of Cheops pyramid. Observations of minute and deep cracks in the microstructure and salt crystallization into. **b** EDX spectrum and micro analysis of the previous image of the limestone grains from the backing stone blocks of Cheops pyramid. A strong Calcium signal is observed. **c** SEM micrographs of limestone from the backing stone blocks of Cheops pyramid. The micrographs show the reaction interfaces, service environment and degradation mechanism of the backing limestone blocks. **d** SEM micrographs of limestone from the backing stone blocks of Cheops pyramid

Specific energy dispersion X-ray analysis

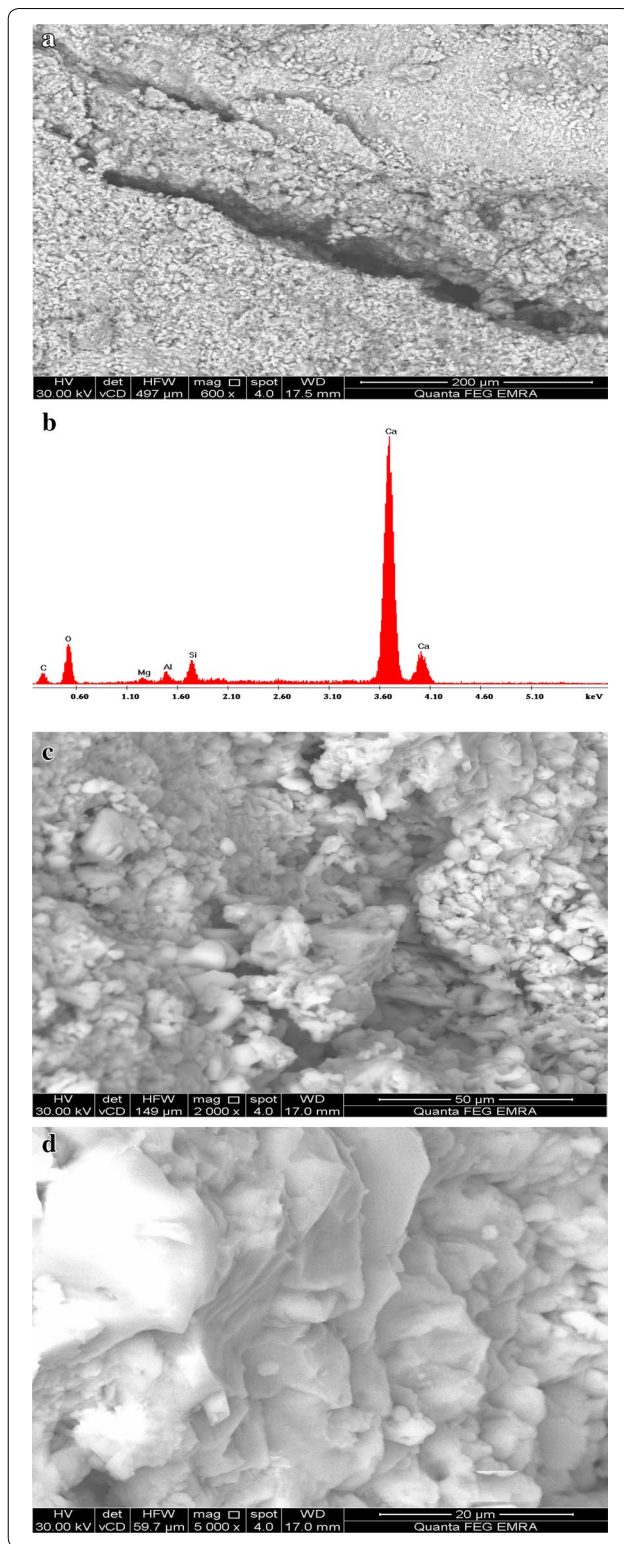
The energy-dispersed X-ray spectrometer (EDS) is a powerful tool for research studies on building materials, particularly structural mortars. Elemental quantification contained in a gypsum mortar microscope can be performed at excellent spatial accuracy. Examination of all samples shows the use of stone fragments in mortar as filler or coarse raw material, and in the relevant EDX analysis showed Ca and Si.

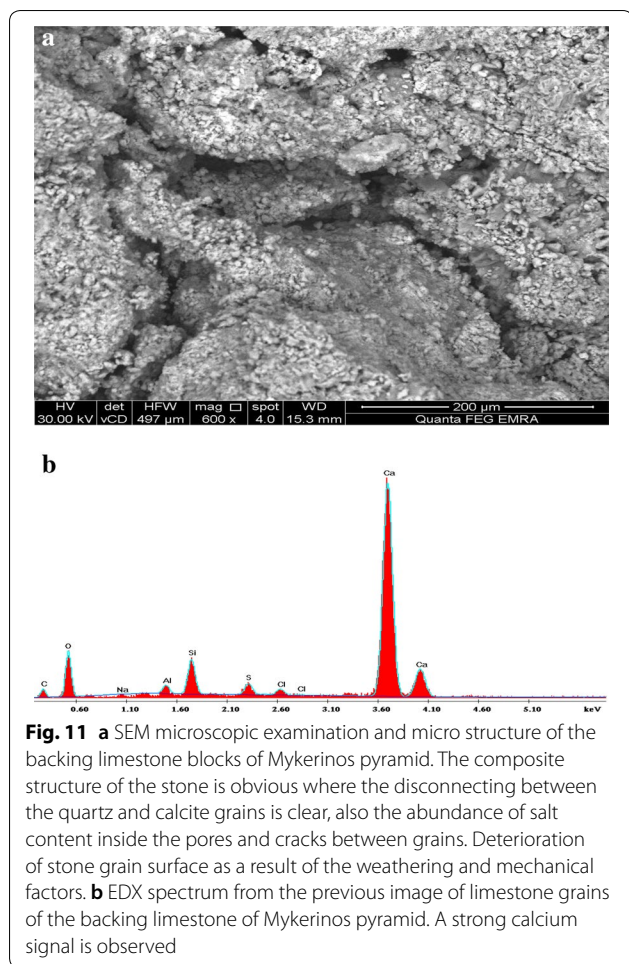
For the structural mortar collected from the pyramids of Cheops and Chephren, the results obtained indicate the presence of Ca, Si, O, S, Cl, Na, and C elements as the main elements in the formation of mortar, suggesting that the structural mortar in these two pyramids is a cannon Gypsum mortar (gypsum and sand), as shown in (Figs. 12b and 14b). In addition to the presence of calcite and iron oxide aggregates, the presence of sodium chloride due to salt contamination (Fig. 14b). The presence of carbon residues and scorched organic matter represented in phosphorus, nitrogen and oxygen P, N, C. While the results obtained from samples collected from the pyramid of Mykerinos revealed that the structural mortar is lime mortar.

The outer casing granite blocks from Mykerinos, pyramid

The morphology of aggregate granite surfaces evaluated by SEM and the results obtained show that the confrontation blocks have been severely affected by various dynamic procedures and physical–chemical action, especially weathering factors that lead to some degradation effects such as: Degradation and fracture of shapes in addition to filling the gaps between grains, (Fig. 15a). The accumulated particles consist of some types of clay minerals and salts. Create red crusts, small cracks and other forms of degradation, (Fig. 15c).

Chemical analyzes of red weathering spots (diameter 3.23 to 50.32 mm) conducted by EDX proved that different proportions of racial oxides are strongly affected but with different degrees according to the location and depth of weathering spots. These results can be summarized as follows:





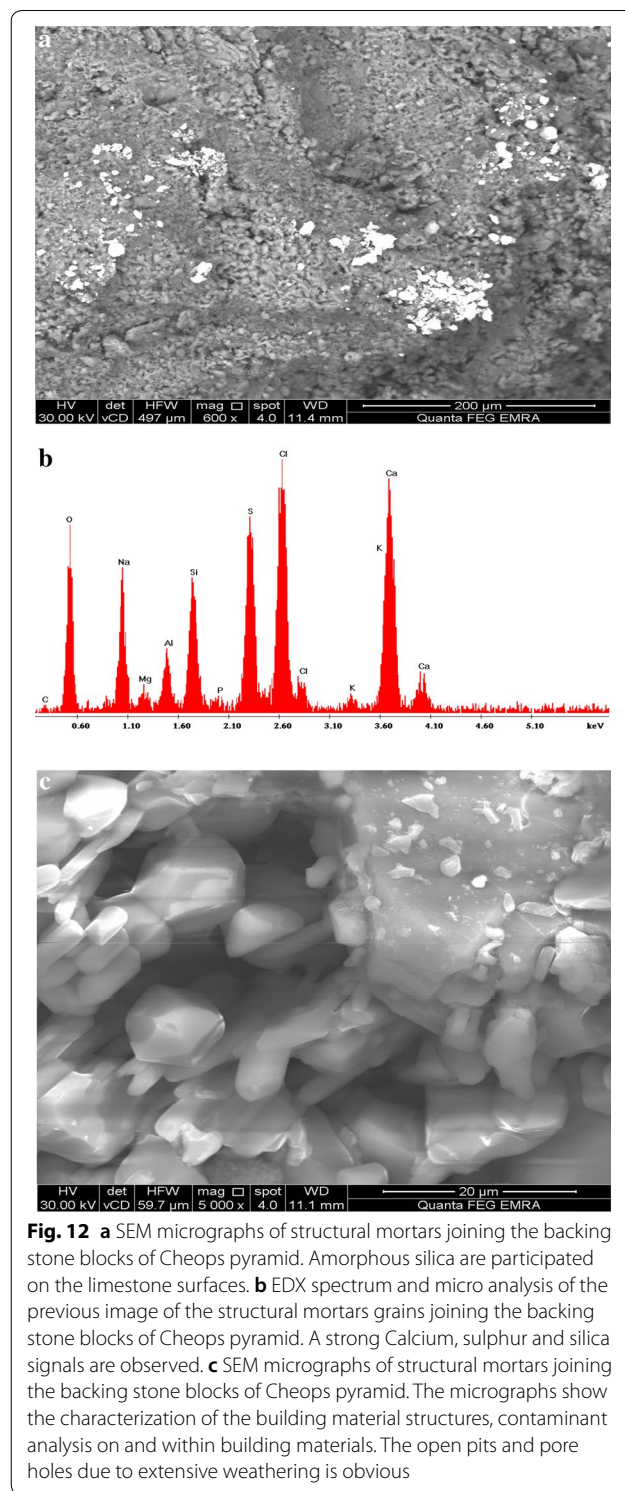
The cortex samples consist of (Si, Al, K, Ca, O, K, Na, C), (Fig. 15b, d).

The primary oxide averages for cortex or crust samples are (SiO₂, 31%), (Al₂O₃, 9%), (K₂O, 21%), (O, 20%), (CaO, 12%) and (NaO, 0.37%).

Thin section analysis under polarizing microscopy (petrographic and mineralogical characteristics)

Thin section analysis was performed to study the cement texture, porosity and permeability. Ten thin sections were prepared for the petrographic study of the sandstone and limestone body and slurry was incorporated to determine the mineral composition and experimental processes of the studied building material samples.

It is important to examine the building materials and the construction of the three great pyramids under polarized light microscopy, to determine the basic type of building materials (building stones and structural mortars) and to identify the original quarries for these stones and building materials. This method relies on polarized light that passes through a thin section of the sample.

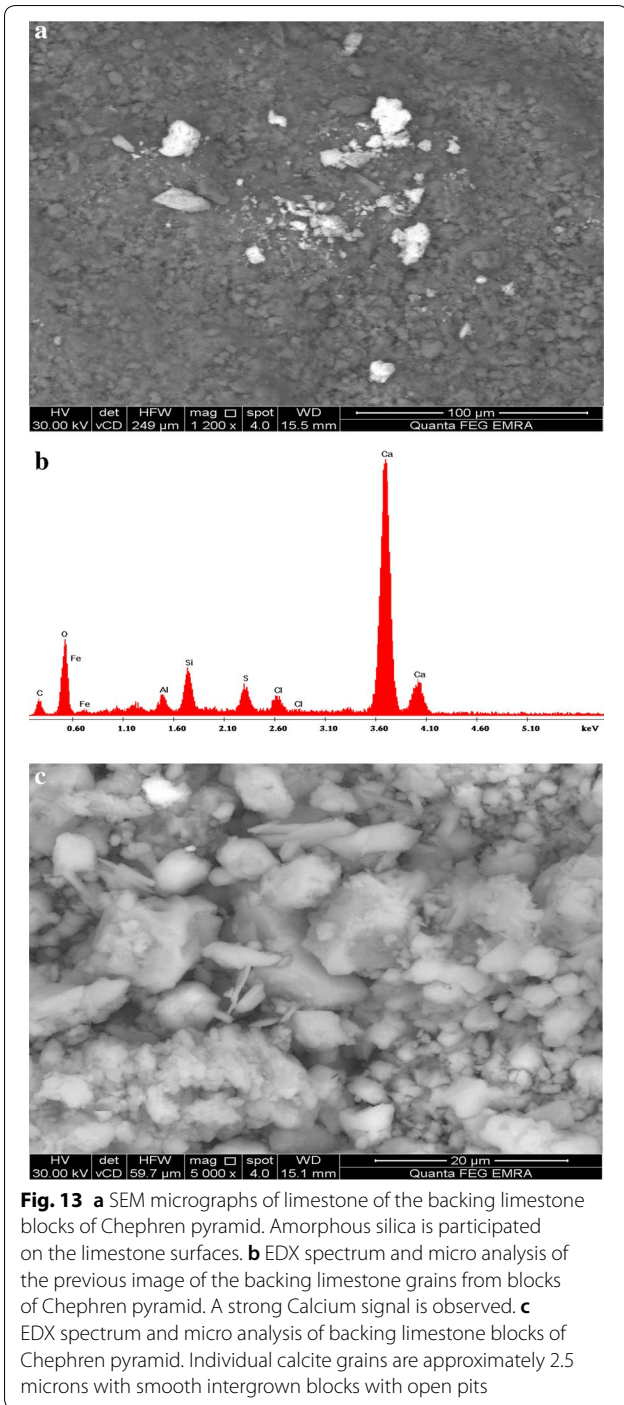


The backing limestone blocks (Cheops, great pyramid)

Rock name: Fossiliferous limestone (Biomicrite).

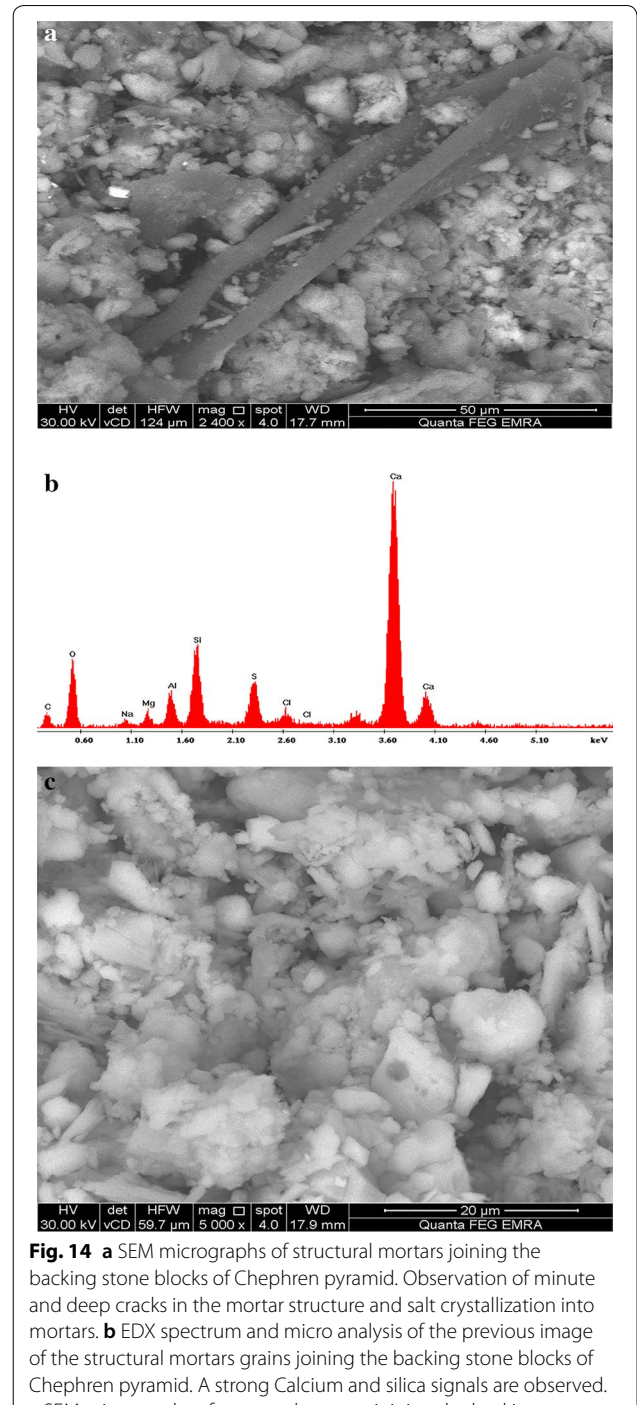
Rock type: Organic, carbonate sedimentary rock.

Texture: The rock is very fine to fine-grained. Micro-fossils of different sizes and shapes are present in a



significant amount, scattered in the rock matrix. Few pore spaces (irregular shapes and sizes) are present in heterogeneous distribution in carbonate matrix of the rock.

Mineral composition: the rock is composed mainly of calcite as the essential component associated with minor amount of iron oxides and quartz and rare of dolomite, opaque minerals and halite.



Calcite represents the majority of the matrix of the rock. It occurs as very fine-grained aggregates, Anhedral crystals interlocked with each other's. Many microfossils of different sizes and shapes are scattered in the matrix of

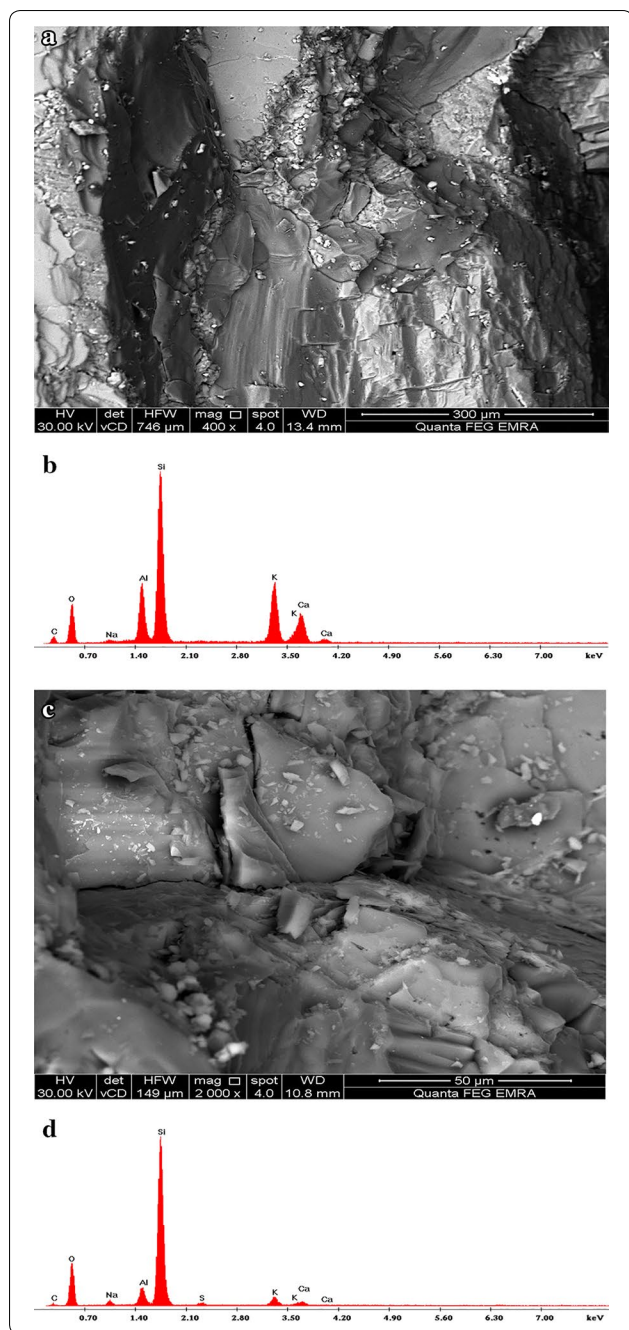


Fig. 15 **a** SEM microscopic examination and micro structure of the outer facing granite blocks of Mykerinos pyramid. Micrographs show heavy materials disintegration and few trace elements are slightly immobile, whereas most major (particularly Ca and Na) and trace elements are mobile from the beginning of the granite weathering. On the other hand, there were mineralogical changes initiated from a plagioclase breakdown, which shows a characteristic circular dissolved pattern caused by a preferential leaching of Ca cation along grain boundaries and zoning. The biotite in that region is also supposed to be sensitive to exterior environmental condition. **b** EDX spectrum of the previous image of the grains of the facing granite blocks of Mykerinos pyramid. A strong silica, aluminum and potassium signals are observed. **c** SEM microscopic examination and micro structure of the facing granite blocks of Mykerinos pyramid. It seems that some rock-forming minerals in the granitic facing blocks are significantly unstable due to the environmental condition. **d** EDX spectrum of the previous image of granite grains of the facing granite blocks of Mykerinos pyramid. A strong silica signal is observed

identify. Occasionally, small nummulites up to 5 mm in length could be recognized at polished surfaces. During storage over a longer period, various salts effloresce at the surface, which can be washed off easily with the finger. With a hand lens, the fossils appear mostly as small nummulites, shells and other fossil remains, all irregularly imbedded and mostly secondarily calcified within the limestone matrix.

The present study confirms that the building stones of the pyramids are natural rocks and were not formed by using artificial concrete.

Structural mortar (Cheops, great pyramid)

Sample Name: Mortar Sample.

Sample Type: Archaeological sample.

Texture: very fine to coarse-grained, showing prophytic texture (fine to coarse-grained of rock fragments

the rock and filled by recrystallized calcite and/or dolomite. Dolomite is very fine to fine-grained, subhedral crystals and associated with calcite. Quartz occurs as fine to very fine-grained Anhedral crystals scattered in the rock. The rock is highly stained by iron oxides in some parts (Fig. 16).

These limestones are of a grey-beige to yellow-brown colour, mostly compact but also porous in places, and they feel chalky due to marly components. Many of small-sized fossil remains are detectable but hard to

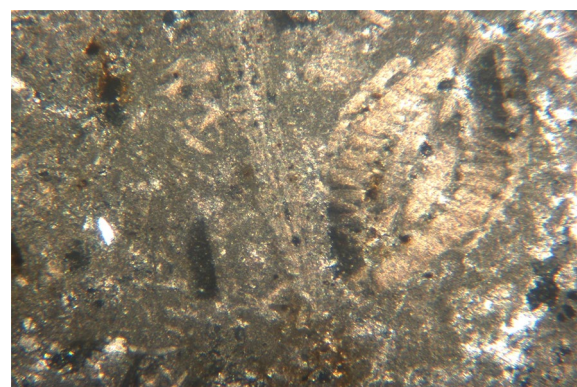


Fig. 16 Microscopic photograph shows the backing Fossiliferous limestone (Biomicrorite) blocks of Cheops pyramid, which composed mainly of calcite as the essential component associated with minor amount of iron oxides and quartz and rare of dolomite, opaque minerals and halite

gypsum, biotite, muscovite and rare quartz grains enclosed in a very fine-grained matrix). Many irregular pore space are detected in the sample.

Mineral composition: The sample is very fine to coarse-grained and composed of gypsum, rock fragments (composed of calcite and dolomite), biotite, muscovite and rare quartz grains cemented by very fine-grained matrix of gypsum, anhydrite, calcite admixed with minor iron oxides. Minor amounts of mafic minerals (biotite and muscovite) and opaque minerals are observed scattered in the sample. Rock fragments are represented by fossiliferous limestone, dolostone, gypsum and anhydrite.

Rock fragments occur as medium to coarse-grained of rounded to subangular outlines, scattered in the sample matrix. Quartz occurs in rare amounts as very fine to fine-grained of rounded to subangular outlines cemented by a mixture of very fine-grained cement matrix. Iron oxides and opaque minerals occur as very fine to medium-grained scattered in the sample. Mafic minerals present as very fine to fine-grained, and observed in the matrix of the sample. Many of irregular pore spaces and cavities are detected in the sample (Fig. 17).

The backing limestone blocks (Chephren's pyramid)

Rock name: Fossiliferous limestone (Biomicrite).

Rock type: Organic carbonate sedimentary rock.

Texture: The sample is very fine-grained. Some microfossils of different sizes and shapes are observed in the rock matrix.

Mineral composition: the rock is very-grained and composed mainly of calcite as the essential component associated with rare amounts of iron oxides, microcrystalline quartz and opaque minerals. Calcite represents the matrix of the rock and occurs as very fine-grained (micrite), anhedral to subhedral interlocked crystals. Quartz is detected as very fine-grained crystals scattered in the matrix. It also presents as aggregates partially and/or completely filling microfossils. Some microfossils of different sizes and shapes are observed scattered in the carbonate matrix. Microfossils are mostly filled by recrystallized calcite. Some pores of irregular shapes and various sizes are observed scattered in the rock. Some parts of the sample are stained by iron oxides (Fig. 18).

Structural mortars (Chephren's pyramid)

Sample Name: Mortar sample.

Sample Type: Archaeological sample.

Texture: very fine to coarse-grained, showing prophyritic texture (fine to medium-grained of quartz, gypsum and rock fragments enclosed in very fine-grained matrix). Significant amounts of irregular pore space are detected in the sample.

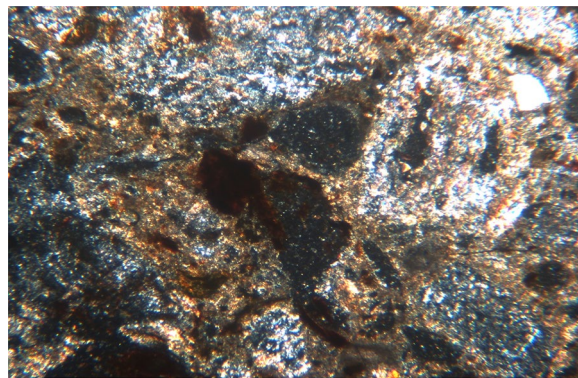


Fig. 17 Microscopic photograph shows the structural mortars joining the backing limestone blocks of Cheops pyramid. The joining mortar is very fine to coarse-grained and composed of gypsum, rock fragments (composed of calcite and dolomite), biotite, muscovite and rare quartz grains cemented by very fine-grained matrix of gypsum, anhydrite, calcite admixed with minor iron oxides

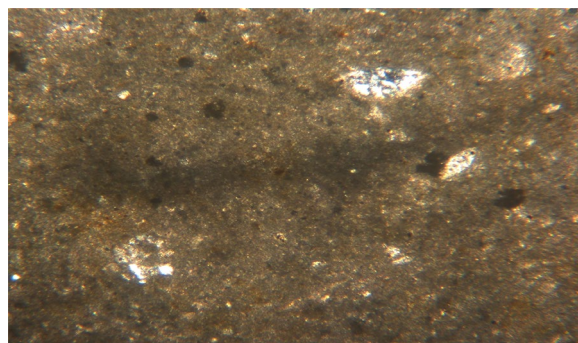


Fig. 18 Microscopic photograph shows the backing Fossiliferous limestone (Biomicrite) blocks of Chephren pyramid. The limestone is very-grained and composed mainly of calcite as the essential component associated with rare amounts of iron oxides, microcrystalline quartz and opaque minerals. Calcite represents the matrix of the rock and occurs as very fine-grained (micrite), anhedral to subhedral interlocked crystals. Quartz is detected as very fine-grained crystals scattered in the matrix

Mineral composition: The sample is composed of gypsum, anhydrite and rock fragments (composed mainly of calcite) associated with minor amounts of quartz, biotite, iron oxides and opaques cemented by very fine-grained matrix of gypsum admixed with calcite, anhydrite, halite and iron oxides. Quartz occurs as fine to medium-grained of rounded to subangular outlines and some of which are cracked. Quartz grains are cemented by a mixture of very fine-grained cement matrix. Rock fragments are represented by limestone, gypsum and anhydrite which occur as medium-grained and rounded to subangular in sample. Iron oxides and opaque minerals

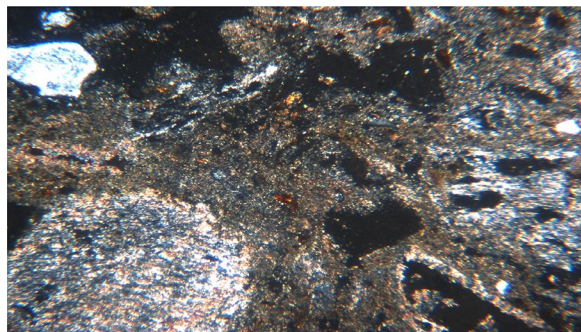


Fig. 19 Microscopic photograph shows the structural mortars joining the backing limestone blocks of Chephren pyramid. Very fine to coarse-grained, showing prophyritic texture (fine to medium-grained of quartz, gypsum and rock fragments enclosed in very fine-grained matrix). Significant amounts of irregular pore space are detected in the sample. The sample is composed of gypsum, anhydrite and rock fragments (composed mainly of calcite) associated with minor amounts of quartz, biotite, iron oxides and opaques cemented by very fine-grained matrix of gypsum admixed with calcite, anhydrite, halite and iron oxides

occur as very fine to medium-grained scattered in the sample. Significant amounts of irregular pore space and cavities (vugs) are detected in the sample (Fig. 19).

The outer casing granite blocks (Mykerinos, pyramid)

Rock name: granite

Rock type: plutonic, acidic igneous rock

Texture: the rock is medium to coarse-grained showing, equigranular, hypidiomorphic, perthitic and piokilitic texture.

Mineral composition: the rock is composed mainly of potash feldspar (microcline, orthoclase and perthite), quartz and plagioclase associated with considerable amounts of hornblende and biotite and accessory amount of muscovite, titanite, zircon and opaque minerals. Secondary minerals are represented by iron oxides sericite and clay minerals. Potash feldspar (microcline, orthoclase and perthite) is the most abundant constituent of the whole rock. It is medium to coarse-grained, generally subhedral to anhedral crystals and slightly altered to clay minerals. Plagioclase replaces and forms fine lamellae (perthitic intergrowths) over microcline showing perthitic texture. Quartz is an essential mineral constituent occurs as fine to coarse-grained, anhedral crystals. It also presents as crystal aggregates that fill in the interstitial spaces between feldspar crystals.

Quartz shows stretched, sutured, fractured and curved boundaries due to mild deformation process. Plagioclase is medium to coarse-grained, subhedral platy in form and shows distinct lamellar twinning. Plagioclase is slightly altered to sericite. It presents also as irregular lamellae,

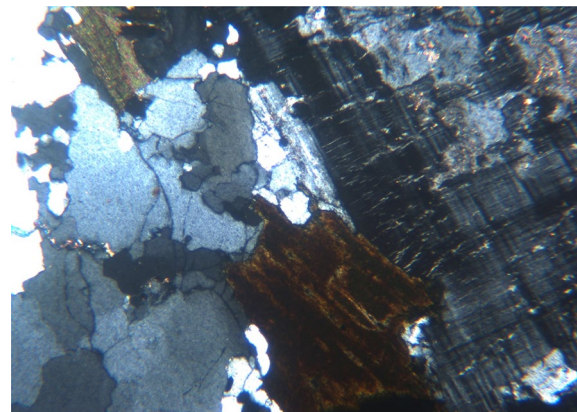


Fig. 20 Microscopic photograph shows the facing granite, plutonic, acidic igneous rock blocks of Mykerinos pyramid. The rock is medium to coarse-grained showing, equigranular, hypidiomorphic, perthitic and piokilitic texture. The rock is composed mainly of potash feldspar (microcline, orthoclase and perthite), quartz and plagioclase associated with considerable amounts of hornblende and biotite and accessory amount of muscovite, titanite, zircon and opaque minerals. Secondary minerals are represented by iron oxides sericite and clay minerals

thin films and fine inclusions intergrowths in microcline perthite. Hornblende presents as fine to medium-grained aggregates, prismatic crystals in association with biotite. Biotite occurs in minor amount as medium to fine-grained aggregates, tabular, flaky crystals at the interstices of feldspars and quartz. It is partially altered to iron oxides (Fig. 20).

Alteration: the rock is affected by mild deformed and slightly alteration. Alteration products are clay minerals and sericite after potash feldspars and plagioclase. Hornblende and biotite are moderately altered to iron oxides. Quartz frequently shows curved boundaries and fractured, stretched and sutured due to mild deformation process.

Opaque minerals: are minor amount, forming fine-grained dissemination in the rock. Opaques show common association with biotite and hornblende.

The backing limestone blocks (Mykerinos, pyramid)

Rock name: Fossiliferous limestone (Biomicrite).

Rock type: Organic, carbonate sedimentary rock.

Texture: The rock is very fine to fine-grained. Significant amount of microfossils of different sizes and shapes are present in the matrix. Few pore spaces (irregular shapes and sizes) are present in heterogeneous distribution in carbonate matrix of the rock.

Mineral composition: the rock is composed mainly of calcite as the essential component associated with minor amount of iron oxides and rare amounts of quartz,

gypsum and opaque minerals. Calcite represents the majority of the matrix of the rock and occurs as very fine-grained aggregates, anhedral crystals interlocked with each other's. Iron oxides occur in considerable amount as fine-grained aggregates and also as patches stained some parts of the sample. Significant amount of microfossils of different sizes and shapes are scattered in the matrix of the rock and filled by recrystallized calcite and/or dolomite. Quartz occurs as fine to very fine-grained Anhedral crystals scattered in the rock. The rock is highly stained by iron oxides (Fig. 21). A somewhat higher porosity can be observed, which is due to the many open fossil inter-spaces. Further, a denser structure of the many small nummulites, discocyclinae, and other fossil remains is evident.

Engineering characterization of the filling limestone blocks from the three pyramids (results and discussion)

Physical properties of the limestone

Determination of the specific fossiliferous limestone weight; the real specific weight using Gibertini E42 scale and pycnometer and the bulk density using Gibertini E42 scale and caliper.

Porosity analysis to determine full open porosity and pore size distribution via water absorption measurements (Thermo Quest Pascal 246 mercury scale; Mercury porosity scale according to UNI—Normal 4/80; Gibertini E42 scale).

Unit weight, specific gravity, water absorption, total and open porosity

Petrophysical properties of the backing limestone blocks samples from the three pyramids: Physical measurements referred that the unit weight (γ) of limestone is between 1.99 and 2.31 g/cm³, Specific gravity (G_s) in range of 1.97 to 2.31, water absorption (W_a) is between 12 and 20% and the total porosity (n) ranged from 21 to 33%. Results are summarized in Table 10. According to the ASTM C568/C568M-15 [33] the physical characteristics of the construction materials of the three pyramids is low, since the water absorption by weigh/max must be in range of 3% for the low density limestone to 12% for the high density limestone.

Pore size distributing/pore media characterization

Five cylindrical specimens of backing limestone blocks were collected from the Khufu pyramid and verified to determine the characterization of pore media for this fossil limestone [29]. Note that: the distribution of the pore diameter of the basic sandstone blocks is, 10–20A (0.15%), 20–30A (0.05%), 30–50A (0.105%), 50–100A

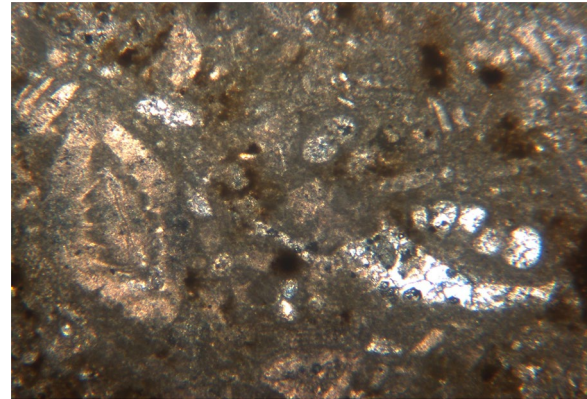


Fig. 21 Microscopic photograph shows the backing Fossiliferous limestone (Biomicroite) blocks of Mykerinos pyramid. The rock is very fine to fine-grained. Significant amount of microfossils of different sizes and shapes are present in the matrix. Few pore spaces (irregular shapes and sizes) are present in heterogeneous distribution in carbonate matrix of the rock. The rock is composed mainly of calcite as the essential component associated with minor amount of iron oxides and rare amounts of quartz, gypsum and opaque minerals. Calcite represents the majority of the matrix of the rock and occurs as very fine-grained aggregates, anhedral crystals interlocked with each other's. Iron oxides occur in considerable amount as fine-grained aggregates and also as patches stained some parts of the sample

(0.09%), 100–200A (0.06%), 200–2330A (96.42%), and $nm = 2.79 \times 10^{-5}$, BET (m²/gr)=2.9, TPV (ml/gr)=1.8, and micro porosity % is 2.77, as shown in Table 10.

Weathering is associated with structural properties, such as weak physical and mechanical properties of geometry, chemical composition, and the presence of soluble salts in porous systems of building stones and structural mortars that are considered the binding agents for building elements in the history of structures. The durability of this limestone is moderate due to the weakness of binding material among the calcite grains. This moderate stone strength seriously affects the integrity of great hierarchical structures under constant and seismic loading conditions [34, 35].

Mechanical properties of the backing limestone

The sample preparation was conducted in accordance with the ASTM standard for uniaxial and tri-axial compressive testing (ASTM D7012-10 (2010)) Standard Test Method for Compressive Strength and Elastic Moduli of Intact Rock Core Specimens under Varying States of Stress and Temperatures [36]. In order to maintain consistency, all the samples were cored to 50 mm in diameter using the same block of Fossiliferous limestone at the same orientation.

Table 10 Petro-physical properties of the backing limestone blocks

Limestone	No.	Unit weight (γ) (g/cm ³)	Specific gravity (Gs)	Open porosity (%)	Total porosity (n) (%)	Water absorption (Wa) %	BET (m ² /gr)	TPV (ml/gr)	Micro Porosity
Cheops' pyramid	1	2.12	2.15	21.39	25	15.70	2.9	1.8	2.77
	2	1.99	2.03	22.99	24	16.76			
	3	2.21	2.19	21.20	23	14.81			
Chephren's pyramid	1	2.31	2.31	20.02	21	12.62	2.7	1.6	2.78
	2	2.29	2.27	19.01	24	13.02			
	3	2.25	2.27	22.02	23	15.20			
Mykerinos' pyramid	1	2.05	2.00	28.24	29	20.88	3.2	2.1	3.42
	2	2.10	2.10	27.08	30	19.05			
	3	2.11	1.97	29.30	33	17.21			

Table 11 Compressive strength, tensile strength, shear strength, longitudinal wave velocity, rebound number, and Toughness Indexes tests results of results of backing limestone blocks, Cheops pyramid

No.	D (mm)	H (mm)	A ² (mm ²)	Failure load (kN)	σ _c (MPa)	σ _t (MPa)	Shear strength (N/mm ²)	V _p (km/s)	(RN) rebound number	Toughness Indexes (AIV test)
1	37.2	78	999.3	15.50	14.34	4.21	1.98	6.34	36	9.80
2	40.2	80	1134.6	13.10	14.76	3.62	1.99	5.30	37	12.90
3	40.2	79	1025.8	14.92	15.48	3.99	1.78	4.88	29	13.00
4	39.2	82	1180.5	15.80	13.43	3.61	2.01	4.77	27	9.01
5	39.3	82	1250.5	11.80	12.65	2.23	1.77	3.88	25	7.30

Uniaxial compressive strength (UCS) and Young's modulus of the backing limestone blocks

Of all the tests carried out, the test of the compressive strength of the stones is very important, as this value is used by structural design engineers to assess the stability and structural conditions. Future research could consider combining the scratch test coupling with the on-site recoil hammer test with greater reliability to evaluate the stones on site without disturbing/destroying structures.

The compressive strength is the maximum load per unit area that the stone can bear without crushing. A higher compressive strength indicates that the stone can withstand a higher crushing load. The required values range from 7569 psi (52 MPa) for marble (ASTM C 503) to 19,000 psi (131 MPa) for granite (ASTM C 615). To determine the compressive strength, at least 5 specimens are tested in ASTM 170. They should be cubes at least 2" to 3" on each side. Each face must be perfectly flat and they must be parallel or perpendicular with each other. Faces must be smooth with no tool marks and there should be no nicks at the corners.

Fifteen samples were equipped with electric strain gauges with a length of 100 mm. Vertical pressure was gradually increased until failure. Table 11 shows the compressive strength results of the five backing

limestone samples collected from the Cheops pyramid. The compressive strength (σ_c) was between 12.14 and 15.16 MPa, indicating medium to poor geochemical characteristics. The average elastic modulus obtained for the five tested cylinders is 12.74 GPa. The results are shown in Table 12. Figure 22 shows the uniaxial and tri-axial compression testing set up.

The results of the compressive strength (σ_c) of the five backing limestone samples collected from the Pyramid of the Chephren are ranged from 12.1 to 17.8 MPa, suggesting medium to poor geomechanical properties. The average elastic modulus obtained for the five cylinders tested is 13.82 GPa. The results are given in Tables 13 and 14.

The results of compressive strength (σ_c) for the five backing limestone samples collected from the Mykerinos pyramid was between 10.20 and 13.08 MPa, suggesting very poor geomechanical properties. The average elastic modulus obtained for the five cylinders tested is 11.57 GPa. The results are given in Tables 15 and 16. The low compressive strength of Mykerinos backing limestone specimens are due to its higher porosity which has been observed by mentioned thin sections. The high porosity may be due to the many open fossil interspaces. Further, a denser structure of the many small nummulites, disco-cyclinae, and other fossil remains is evident and reduced

Table 12 Modulus of Elasticity backing limestone blocks, Cheops pyramid

No.	Strain at 0.5 Mpa ($\times 10^{-6}$)	Ultimate strength f_{ult} (MPa)	Strain at $f_{ult}/3$ ($\times 10^{-6}$)	Modulus of Elasticity (GPa)	Remarks
1	9	10.2	320	14.100	
2	10	14.12	341	15.182	
3	11	15.23	419	14.940	

So the average value for Modulus of Elasticity = 12.74 GPa



Fig. 22 Uniaxial and triaxial compression test set up

its stiffness and strength, (see Fig. 23). According to the ASTM C 170, C 880, C 99 test methods and ASTM C568/C568M-15 specifications [33] the physical and mechanical characteristics of the construction materials of the three pyramids is low, since the standard requirement for

the uniaxial compressive strength (σ_c) of the limestone must be in range of 12 MPa for the low density limestone to 55 MPa for the high density limestone. The physical and mechanical properties of the construction materials of the three great pyramids are retreated because the area was subjected to intensive seasonal rainfall and evaporation in temperature (Mediterranean) climate conditions.

The experimental study indicates the dependence of mechanical geological properties on the physical properties and the mineral composition of the studied building materials. The physical and petrographic characteristic of the stones are related. The modeling of properties indicates a reliable relationship between the various visible pores and uniaxial compression force parameters that can be applied to predict and characterize limestone formations elsewhere.

Splitting tensile strength of the backing limestone blocks

Fifteen cylinders were tested to determine the average split tensile strength of the fossil limestone of the three great pyramids. The split tensile strength of the collected backing limestone specimens from of the great pyramid of Khufu is ranges from 1.99 to 3.71 MPa. The limestone tensile strength of the collected backing limestone specimens from of the pyramid of Chephren pyramid ranges from 1.79 to 3.71 MPa. The limestone tensile strength of the collected backing limestone specimens collected from the pyramid of Mykerinos is ranges from 2.23 to 2.98 MPa. Tables 11, 13 and 15 give details of test results.

Shear strength of the backing limestone blocks

Fifteen cylinders were tested in single shear to determine the shear strength parameters of the filling limestone from the three great pyramids. The obtained shear strength for the backing limestone from Cheops pyramids equal 1.77 to 2.01 MPa. The obtained shear strength for the backing limestone from Chephren pyramid equal 1.67 to 2.28 MPa. The obtained shear strength for the backing limestone from Mykerinos pyramid equal 0.89 to

Table 13 Compressive strength, tensile strength, shear strength, longitudinal wave velocity, rebound number, and Toughness Indexes tests results of results of backing limestone blocks, Chephren pyramid

No.	D (mm)	H (mm)	A ² (mm ²)	Failure load (kN)	σ_c (MPa)	σ_t (MPa)	Shear strength (N/mm ²)	Vp (km/s)	(RN) rebound number	Toughness Indexes (AIV test)
1	37.7	70	1000.3	14.50	16.14	3.21	1.91	5.06	32	11.50
2	38.2	76	1014.6	13.10	15.66	2.02	2.09	5.31	36	10.90
3	36.2	74	1012.8	15.22	17.78	3.71	2.28	6.80	29	11.99
4	38.2	76	1200.1	16.30	13.60	1.99	2.18	4.80	24	8.2
5	39.2	73	1207.5	16.80	12.79	1.49	1.67	4.50	25	8.1

Table 14 Modulus of Elasticity backing limestone blocks, Chephren pyramid

No.	Strain at 0.5 Mpa ($\times 10^{-6}$)	Ultimate Strength f_{ult} (MPa)	Strain at $f_{ult}/3$ ($\times 10^{-6}$)	Modulus of Elasticity (GPa)	Remarks
1	10	11.92	340	12.600	
2	9	12.42	359	13.892	
3	9	12.31	348	14.980	

So the average value for Modulus of Elasticity = 13.82 GPa

1.46 MPa. Tables 11, 13 and 15 summarize the results of shear test.

Ultrasonic longitudinal wave velocity (Vp) measurements

Ultrasonic pulse velocity testing, mainly used to measure the sound velocity of the stones and hence the compressive strength of the stones. Measurement of longitudinal sound wave velocity can be an indication of the depth of crack observed on the surface. The aim of the study here was to associate the velocity of sound with different mechanical properties [37].

P-wave velocities were measured by the Pundit (CNS portable non-destructive ultrasonic indicator tester), which has two 65 kHz transducers (transmitter and receiver).

The backing limestone samples of the Cheops pyramid recorded low speed (3.88–6.34 km/s), as indicated in Table 11. Limestone samples from the Chephren pyramid recorded low speed (4.5–6.8 km/s), indicated in Table 13 recorded limestone samples from the Mykerinos pyramid at low speed, (3.76–5.26 km/s), as is shown in Table 15. Figure 24 represent the test results.

Modeling of the characteristics as shown in Fig. 24 indicates a reliable relationship between longitudinal velocity waveform parameters (Vp) and uniaxial pressure resistance parameters (σ_c) which can be applied to predict and characterize weathered limestone elsewhere.

Table 15 Compressive strength, tensile strength, shear strength, longitudinal wave velocity, rebound number, and Toughness Indexes tests results of backing limestone blocks Mykerinos pyramid

No.	D (mm)	H (mm)	A ² (mm ²)	Failure load (kN)	σ_c (MPa)	σ_t (MPa)	Shear strength (N/mm ²)	Vp (km/s)	(RN) rebound number	Toughness Indexes (AIV test)
1	35.7	68	990.3	13.50	13.11	2.70	0.89	5.26	25	9.50
2	37.2	70	1034.6	12.10	12.23	1.99	1.33	5.10	22	8.80
3	35.2	69	922.8	14.22	13.28	2.98	1.46	4.97	20	9.80
4	37.2	72	1180.1	14.30	12.20	2.11	1.22	4.67	19	7.01
5	37.2	72	1150.5	15.80	10.79	1.79	1.11	3.76	17	6.24

Table 16 Modulus of Elasticity for of backing limestone blocks Mykerinos pyramid

No.	Strain at 0.5 Mpa ($\times 10^{-6}$)	Ultimate strength f_{ult} (MPa)	Strain at $f_{ult}/3$ ($\times 10^{-6}$)	Modulus of Elasticity (GPa)	Remarks
1	9	9.2	290	12.200	
2	9	10.22	353	11.172	
3	8	11.31	279	11.350	

So the average value for Modulus of Elasticity = 11.57 GPa

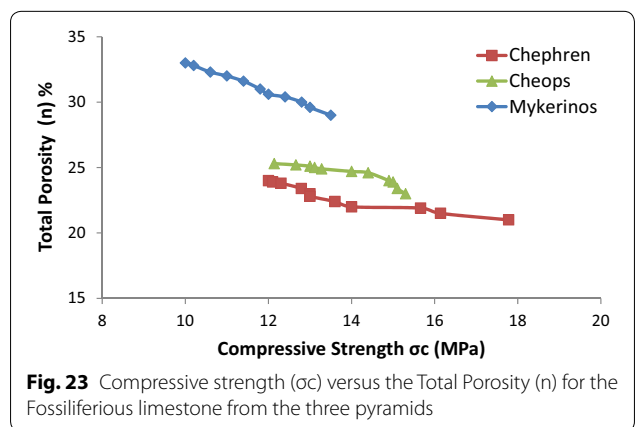


Fig. 23 Compressive strength (σ_c) versus the Total Porosity (n) for the Fossiliferous limestone from the three pyramids

Schmidt hammer rebound number (RN)

In general, the rebound hammer is used to determine the quality of concrete and rock formations [38, 39]. The Schmidt hammer method is one of the nondestructive testing techniques and is frequently adopted for evaluating the quality of in situ historic masonry structures. Whereas in this study, an attempt was made to assess the local compressive strength of limestone as a measure of the non-destructive test method. This approach requires extensive study and will be useful in the long term to test the heritage structures made of stones [40, 41].

The Schmidt L-Type hammer of impact energy of 0.74 NM was used in this work. The hammer was transferred and 30 effects were performed on each sample.

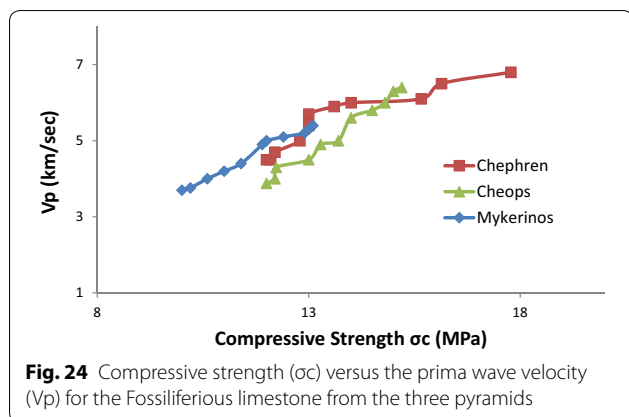


Fig. 24 Compressive strength (σ_c) versus the prima wave velocity (V_p) for the Fossiliferous limestone from the three pyramids

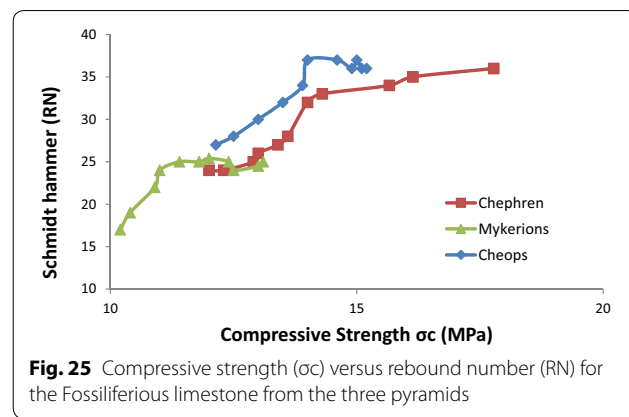


Fig. 25 Compressive strength (σ_c) versus rebound number (RN) for the Fossiliferous limestone from the three pyramids

The hammer is forced against the surface of the stone block by the spring and the distance of rebound is measured on a scale. The test surface was horizontal and vertical. The rebound hammer test is described in ASTM C 805-85 [42]. Rebound Hammer test was carried out on selected structural backing limestone blocks. It serves as a tool to compare the strength of the existing structures. It gives a good indication on the limestone blocks surface hardness, which is reflective of the stone surface quality and strength.

The geochemical properties of the samples are medium and all are closely related. The values of the Schmidt hammer for the backing limestone blocks of the Khufu pyramid vary between RN 25 and 37; the results are given in Table 11.

The geochemical properties of the samples are medium and all are closely related. The values of the Schmidt hammer for the backing limestone blocks of the Chephren pyramid vary between RN 24 and 36; the results are given in Table 13.

The geochemical properties of the samples are medium and all are closely related. The values of the Schmidt hammer for the backing limestone blocks of the Mykerinos pyramid vary between RN 17 and 25; the results are given in Table 15.

The modeling of the characteristics as shown in (Fig. 25) indicates a reliable relationship between the number of recoil and uniaxial compression force parameters that can be applied to predict and characterize hollow limestone elsewhere.

Impact value (AIV) test

AIV was used as a standard test by which the aggregate impact strength was achieved. As in the Protodyakonov test, the material used consists of irregularly shaped particles of fraction with a size of $- 14 + 10$ mm.

Fifteen tested limestone samples from the three pyramids are exposed to 15 hammer hits falling 380 mm, at

an interval of at least one second. AIV method is better than Protodyakonov to predict “rough” the strength of the impact of rocks.

The shock strength of 15 hammer drops (drops) recorded very low values below 13 indicating poor limestone of the backing blocks of the Khufu pyramid, as shown in Table 11. The impact strength of 15 hammer drops (drops) recorded very low values below 12 indicating poor limestone for the backing blocks of the Chephren Pyramid, as shown in Table 13.

The shock strength of 15 hammer drops (drops) recorded low values below 9 indicating poor limestone for the backing stone blocks of the Mykerinos pyramid, as shown in Table 15).

Modeling of the characteristics as shown in Fig. 26 indicates a reliable relationship between Toughness indexes (AIV test) and uniaxial pressure resistance parameters (σ_c) which can be applied to predict and characterize weathered limestone elsewhere.

Physical characterization of the structural mortars

Table 17 summarizes the main physical characteristics of the joining mortars between backing limestone blocks from the three great pyramids. The determined physical characterization includes the aggregate maximum size (mm), proportion mortar to aggregate and the fines < 0.075 mm (%).

For the Capillarity Coefficient of structural mortars, the samples were first submitted to the water absorption tests using the technique of capillary absorption by contact, which was developed and calibrated previously. The capillarity coefficient obtained by this test gives an idea of the compacity and consequently of the state of conservation of samples. Moreover, it is a non-destructive test introducing no changes to historic samples. The main results are summarized in Table 18.

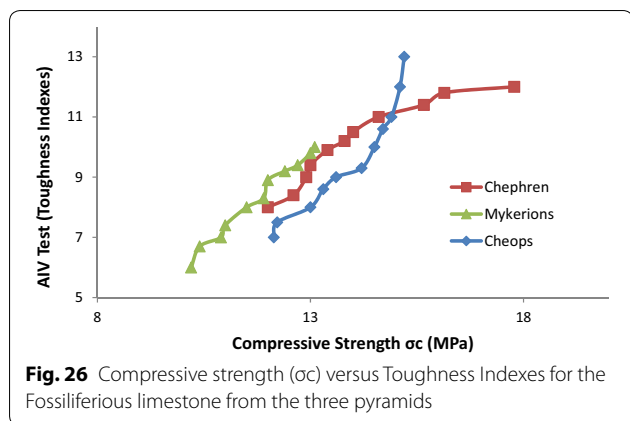


Fig. 26 Compressive strength (σ_c) versus Toughness Indexes for the Fossiliferous limestone from the three pyramids

Table 17 Physical characteristics of aggregates for the structural mortars

Pyramid	Mortars type	Aggregate max size (mm)	Proportion mortar to aggregate	Fines < 0.075 mm (%)
Cheops	Gypsum mortar	12	1:2.2	42.21
		10	1:2.2	31.15
		12	1:2.1	40.22
		13	1:2.2	37.23
		11	1:2.1	39.24
		10	1:2.2	32.21
		13	1:2.2	32.31
Chephren	Gypsum mortar	12	1:2.2	40.51
		13	1:3.2	33.22
		14	1:3.2	35.31
		16	1:3.2	24.42
		16	1:2.1	28.51
Mykerinos	Lime based mortar	17	1:2.2	31.31
		16	1:2.2	30.21
		18	1:2.2	22.42
		20	1:2.1	23.41
		18	1:3.2	33.32
		25	1:2.3	35.21
		22	1:3.2	38.81

Table 18 Capillarity coefficient the structural mortars

Mortars	Capillarity coefficient ($\text{kg/m}^2 \text{h}^{1/2}$)		
	C90-10 S	Ccc5 NS	C90-10 NS
Cheops	9.5	10.2	6.4
Chephren	8.1	9.3	5.1
Mykerinos	8.3	9.2	4.4

Conclusions

The pyramids complex suffered from different types of structural damage and construction materials decay and disintegration. The sources of this degradation can generally be classified as: nature, time, and man-made. In recent years, the great pyramids of the 4500-year-old at Giza plateau, Cheops (Khufu), Chephren (Khafre), Mykerinos (Menkaure) and the Great Sphinx have been threatened by rising groundwater levels caused by water infiltration from the suburbs, Irrigation canals and mass urbanization surrounding Giza pyramids plateau GPP.

The presence of building materials under investigation with great physical sensitivity to structural damage and weathering factors, especially dynamic procedures and high seismic events.

This study involved collection of intact stones and mortars samples without any damage but scattered on the floor; in situ testing of intact stones on the standing walls using non-destructive tests and carrying out laboratory testing of collected stone samples for assessment of strength characteristics. The multi-criteria analysis allowed the integration of several elements to map areas and zones at risk.

The detailed analytical study proved that these pyramids complexes are built of natural building materials, for the three pyramids complex, the filling or backing stones blocks are Fossiliferous limestone had been quarried and transported from Giza quarries that lie only a couple of 100 m south of the great pyramid, east of Khafre and south-east of the Mynkaure pyramid. The rock-cut trench west and north of the Khafre pyramid yielded an enormous amount of stone material, which was incorporated directly into the core masonry. The outer casing stone blocks for Cheops, great pyramid are white fine limestone were quarried and transported from Mokkatam Formations in particular from Tura quarry. The outer casing stone blocks for the Chephren’s pyramid is very fine limestone were quarried and transported from the Tura- Mssara quarries, Only a fraction of the original casing remains on the uppermost parts of the building. The outer casing stone blocks for the Mykerinos, pyramid is granite was imported from Aswan quarry. In contrast to the Khufu pyramid, which was most probably entirely covered with limestone blocks, the Khafre pyramid’s base layers were cased with blocks of various granite types from the large quarry area south of Aswan. The structural mortars joining the backing stone blocks of Cheops and Chephren pyramids are Gypsum mortars while is lime based mortar for the Mykerinos pyramid. The present study confirms that the building stones of the pyramids are natural rocks and were not formed by using artificial concrete. The most of the casing stone blocks were destroyed and fell down in the 1303 A.C

earthquake and were reused for the construction of many Coptic and Islamic historic buildings in Cairo.

The study presented a detailed view of the geochemical and engineering properties of the materials used in the construction of the three pyramids complex (stones and structural mortars) and the weathering and erosion factors that affect their durability and sustainability. All construction materials offer low physical and mechanical characteristics, which may affect the structure's safety factors for static and seismic loading at the lower levels. The present study indicates the dependence of mechanical properties on the physical and petrochemical properties of the studied building materials. Character modeling indicates a reliable relationship between different parameters.

The study revealed the existence of an original hill of large volume under the two great pyramids. The volume of this original hill is about 11.5% for the pyramid of Khephren and about 23% for the pyramid of Kheops.

The experimental study indicates the dependence of mechanical geological properties on the physical properties and the mineral composition of the studied building materials. The physical and petrographic characteristic of the stones are related. The modeling of properties indicates a reliable relationship between the various visible pores and uniaxial compression force parameters that can be applied to predict and characterize limestone elsewhere.

Further site investigations are required to assess foundation details, bearing capacity and stability calculations for each section or segment of the pyramid complex. Concentrated strengthening and structural retrofitting intervention are therefore essential and necessary for preservation of the pyramids complex. The structural and non-structural measures recommended in this research will help decision makers and planners to develop effective site management strategies in the future, modify the modernization and structural rehabilitation of this unique archaeological site.

A perched groundwater table might exist in the elevated area toward the west and southwest. Great care must be taken regarding the impact of mass urbanization in the western Great Pyramids of Giza, which may affect the groundwater model in the region, (see Fig. 2).

List of symbols and abbreviations

Symbols

γ_b : Bulk unit weight; γ_d : Dry unit weight; σ_c : Uniaxial compressive strength; σ_{sp} : Splitting tensile strength; V_p : Prima wave velocity; V_s : Shear wave velocity; σ_v : Vertical stress; σ_p : Strength of the pillar; q_u : UCS strength; β : Angle between the normal to the fracture plane and the horizontal plane; φ : Friction angle of the fracture; τ_t : Shear stress in resin annulus; σ_b : Applied stress; α : Decay coefficient 1/in which depends on the stiffness of the system; β : Reduction coefficient of dilation angle; ϕ_b : Basic joint friction angle; U : The shear displacement at each step of loading; c : Cohesion between block joints; σ_n : Normal force; b_u : Shear displacement; N_p : Normal force at failure; Q_p : Shear force at failure;

MD: Bending moment at yield limit; Mp: Bending moment at plastic limit; Ei: Modulus of elasticity of intact rock; Qcf: Shear force; Lcp: Reaction length; v: Poison ration of rock mass; Po: In situ stress.

Abbreviations

XRD: X-ray diffraction; SEM: Scanning electron microscopy; EDX: Energy dispersive X-ray; BET: Brunauer–Emmett–Teller; TPV: Total porosity volume; RN: Rebound number; AIv: Toughness Index; JRC: Joint roughness coefficient; JCS: Joint compressive strength; Q: Rock mass quality.

Acknowledgements

Not applicable.

Authors' contributions

The whole database construction and analysis are presented in the manuscript had been achieved by the first author. All stone samples provided by the second author. All authors read and approved the final manuscript.

Funding

The authors confirm that he is not currently in receipt of any research funding relating to the research presented in this manuscript.

Availability of data and materials

Data sharing not applicable to this article as no datasets were generated or analyzed during the current study.

Competing interests

The authors declare that they have no competing interests.

Author details

¹ Conservation Department, Faculty of Archaeology, Cairo University, PO 12613, Giza, Egypt. ² Ministry of Tourism and Antiquities, Cairo, Egypt.

Received: 14 October 2019 Accepted: 23 January 2020

Published online: 30 January 2020

References

- Lehner M, Hawass Z. Giza and the pyramids. London: Thames and Hudson; 2017.
- Lehner M. The complete pyramids. Solving the ancient mysteries. London: Thames & Hudson Ltd.; 1997.
- Fakhry A. The pyramids. 2nd ed. Chicago: University of Chicago Press; 1969.
- Agaiy SW, El-Ghamrawy MK, Ahmed SM. Learning from the past: the Ancient Egyptians and geotechnical engineering. In: Proc. 4th international seminar on forensic geotechnical engineering, Bengaluru, India. 2013.
- Klemm D, Klemm R. The stones of the Pyramids. Provenance of the Building Stones of the Old Kingdom Pyramids of Egypt. Berlin: German Archaeological Institute Cairo Department, Walter de Gruyter GmbH; 2010.
- Hemdan G. Egypt's identity, a study in the genius of the place. Four volumes. Cairo: Dar el-Helal Publications; 1984. p. 1975–84.
- Sharafeldin MS, Essa KS, Youssef MA, Karsli H, Diab ZE, Sayil N. Shallow geophysical techniques to investigate the groundwater table at the Great Pyramids of Giza, Egypt. Geosci Instrum Method Data Syst. 2019;8:29–43. <https://doi.org/10.5194/gi-8-29-2019>.
- Hemeda S, Fahmy A, Sonbol A. Geo-environmental and structural problems of the first successful true pyramid, (Snefru Northern Pyramid) in Dahshur, Egypt. Geotech Geol Eng. 2019;37:2463–84. <https://doi.org/10.1007/s10706-018-00769-x>.
- Raynaud S, de la Boisse H, Makroum F, Bertho J. Geological and geomorphological study of the original hill at the base of Fourth Dynasty Egyptian monuments. Etude géologique et géomorphologique de la colline originelle à la base des monuments de la quatrième dynastie égyptienne. 2008. hal-00319586ff. <https://hal.archives-ouvertes.fr/hal-00319586/document>.

10. Mahmoud SS. Pyramids plateau, landforms and problems, Geographic Research Series. Cairo: Egyptian Geographic Society; 1997.
11. Dowidar HM, Abd-Allah AMA. Structural setting of the Giza pyramids plateau and the effect of fractures and other factors on the stability of its monumental parts, Egypt. *Ann Geol Surv.* 2001;XXIV:393–412.
12. Omara SM. The structural features of the Giza pyramids area. Ph.D. thesis, University of Cairo. 1952.
13. Yehia MA. Geologic structures of the Giza pyramids plateau. *Sci Res Ser.* 1985;5:100–20.
14. El Aref MM, Refai E. Paleokarst processes in the Eocene limestones of the Pyramids Plateau, Giza, Egypt. *J Afr Earth Sci.* 1987;6:367–77.
15. Petri F. Pyramids and temples of Gizeh. London: Field & Tuer; 1883.
16. Eyth M. Der Kampf um die Cheopspyramide. Heidelberg: Carl Winter's Universitätsbuchhandlung; 1908.
17. Dormion G. La chambre de Chéops: Fayard, Paris. 2004.
18. Badawy A. Historical seismicity of Egypt. *Acta Geodaetica et Geophysica Hungarica.* 1999;34:119–35.
19. Morsy S, Halim M. Reasons why the great pyramids of Giza remain the only surviving wonder of the ancient world: drawing ideas from the structure of the Giza pyramids to nuclear power plants. *J Civil Eng Archit.* 2015;9:1191–201. <https://doi.org/10.17265/1934-7359/2015.10.007>.
20. Jia J. Soil dynamics and foundation modeling: offshore and earthquake engineering. Heidelberg: Springer; 2016.
21. Krishna AM, Bhattacharya S, Choudhury D. Seismic requalification of geotechnical structures. *Indian Geotech J.* 2014;44:113–8. <https://doi.org/10.1007/s40098-014-0115-5>.
22. Ansell R, Taber J. Caught in the crunch: earthquakes and volcanoes in New Zealand. Auckland: HarperCollins; 1996.
23. Ambraseys NN. On the seismicity of the South-West Asia (date from a XV century Arabic manuscript). *Revue pour L'étude calamités, Genève.* 1961;37:18–30.
24. Maraveas C. Assessment and restoration of an earthquake-damaged historical masonry building. *Front Built Environ.* 2019;5(112):1–16. <https://doi.org/10.3389/fbuil.2019.00112>.
25. El-Hadidy SA, Moustafa SSR, Wasef MGS, Mohamed AME, Abu El-Ata AS, Albert RN. Evaluation of liquefaction potential associated with the 1992 Dahshour earthquake, Egypt. *Bull Faculty Sci Zagazig Univ.* 2007;29:447–63.
26. Fergany EA, Sawda S. Estimation of ground motion at damaged area during 1992 Cairo earthquake using empirical green's function. *Seismol Res Lett.* 2009;80:81–8.
27. Kebeasy R, Maamoun M, Albert R, Megahed A. Earthquakes activity and earthquake risk around Alexandria. *Jpn Bull Liege.* 1981;19:93–113.
28. Sykora W. Examination of existing shear wave velocity and shear modulus correlations in soils. Vicksburg: U.S. Army Engineer Waterways Experiment Station; Springfield, Va.: Available from National Technical Information Service. 1987.
29. Maamoun M, Allam A, Megahed A, Abu El-Atta A. Neotectonic and seismic regionalization of Egypt. *Bull IISEE.* 1980;18:27–39.
30. Heyman J. The stone skeleton. *Int J Solids Struct.* 1966;2:249–52.
31. El-Arabi N, Fekri A, Zaghoul EA, Elbeih SF, Laake A. Assessment of groundwater movement at Giza pyramids plateau using GIS techniques. *J Appl Sci Res.* 2013;9:4711–22.
32. Yasseen A. Architecture of the great pyramid of Giza concept and construction. International Journal on: Proceedings of Science and Technology, Alexandria, IEREK press. 2018.
33. ASTM Standard C568/C568M. Standard specification for limestone dimension stone. West Conshohocken: ASTM International; 2003. 2015. https://doi.org/10.1520/c0568_c0568m-15.
34. Hemeda S, Pitolakis K. Serapeum temple and the ancient annex daughter library in Alexandria, Egypt: geotechnical–geophysical investigations and stability analysis under static and seismic conditions. *Eng Geol.* 2010;113:33–43.
35. Ceccconi M, Viggiani GM. Structural features and mechanical behaviour of a pyroclastic weak rock. *Int J Numer Anal Meth Geomech.* 2001;25:1525–57.
36. ASTM D7012-10. Standard test method for compressive strength and elastic moduli of intact rock core specimens under varying states of stress and temperatures. West Conshohocken: ASTM International; 2010.
37. Hemeda S. Geotechnical and geophysical investigation techniques in Ben Ezra Synagogue in Old Cairo area, Egypt. *Herit Sci.* 2019;7:23. <https://doi.org/10.1186/s40494-019-0265-y>.
38. Katz O, Reches Z, Roegiers JC. Evaluation of mechanical rock properties using a Schmidt Hammer, Technical Note. *Int J Rock Mech Min Sci.* 2000;37:723–8.
39. Saptono S. Pengembangan Metode Analisis Stabilitas Lereng Berdasarkan Karakterisasi Batuan di Tambang Terbuka Batubara. Disertasi Doktor, Rekayasa Pertambangan, Institut Teknologi Bandung. 2012.
40. Hemeda S. Engineering failure analysis and design of support system for ancient Egyptian monuments in Valley of the Kings, Luxor, Egypt. *Geoenviron Disasters.* 2018;5:12. <https://doi.org/10.1186/s40677-018-0100-x>.
41. Hemeda S. 3D finite element coupled analysis model for geotechnical and complex structural problems of historic masonry structures: conservation of Abu Serga church, Cairo, Egypt. *Herit Sci.* 2019;7:6. <https://doi.org/10.1186/s40494-019-0248-z>.
42. ASTM C 805-85. Test for rebound number of hardened concrete, ASTM, USA, 1993.

Publisher's Note

Springer Nature remains neutral with regard to jurisdictional claims in published maps and institutional affiliations.

Submit your manuscript to a SpringerOpen[®] journal and benefit from:

- Convenient online submission
- Rigorous peer review
- Open access: articles freely available online
- High visibility within the field
- Retaining the copyright to your article

Submit your next manuscript at ► [springeropen.com](https://www.springeropen.com)